X-480-73-114
PREPRINT

NASA TM X- 66267

IN-ORBIT PERFORMANCE OF THE ITOS IMPROVED ATTITUDE CONTROL SYSTEM WITH HALL GENERATOR BRUSHLESS MOTOR AND EARTH-SPLITTING TECHNIQUE

(NASA-TM-X-66267) IN-ORBIT PERFORMANCE OF THE ITOS IMPROVED ATTITUDE CONTROL SYSTEM WITH HALL GENERATOR BRUSHLESS MOTOR AND EARTH-SPLITTING TECHNIQUE (NASA) 43 p HC $4.25 CSCL 22B G3/21
N73-26662
Unclas
07461

MARCH 1973

GSFC

GODDARD SPACE FLIGHT CENTER
GREENBELT, MARYLAND

Reproduced by
NATIONAL TECHNICAL INFORMATION SERVICE
US Department of Commerce
Springfield, VA. 22151

X-480-73-114

IN-ORBIT PERFORMANCE OF THE ITOS IMPROVED ATTITUDE CONTROL SYSTEM WITH HALL GENERATOR BRUSHLESS MOTOR AND EARTH-SPLITTING TECHNIQUE

William M. Peacock
ITOS Project

March 1973

GODDARD SPACE FLIGHT CENTER
Greenbelt, Maryland

IN-ORBIT PERFORMANCE OF THE ITOS IMPROVED ATTITUDE CONTROL SYSTEM WITH HALL GENERATOR BRUSHLESS MOTOR AND EARTH-SPLITTING TECHNIQUE

William M. Peacock
ITOS Project

ABSTRACT

The National Aeronautics and Space Administration (NASA), Goddard Space Flight Center (GSFC), launched ITOS-D (NOAA-2)* with an improved attitude control system from the Air Force Western Test Range (AFWTR) at Vandenberg Air Force Base, California, on October 15, 1972. A Hall generator brushless dc torque motor replaced the brush dc torque motor on TIROS-M (ITOS-1)** and ITOS-A (NOAA-1).† Two CO_2 attitude horizon sensors and one mirror replaced the four wide-band horizon sensors and two mirrors on ITOS-1 and NOAA-1. Redundant pitch-control electronic boxes containing additional electronic circuitry for earth-splitting and brushless motor electronics were used. A new method of generating a spacecraft earth-facing side reference for comparison to the time occurrence of the earth-splitting pulse was used for the first time to automatically correct pitch-attitude error. A single rotating flywheel, supported by a single bearing, provided gyroscopic stability and the required momentum interchange to keep one side of the satellite facing the earth. Magnetic torquing against the earth's magnetic field eliminated the requirement for expendable propellants which would limit satellite life in orbit.

---

*ITOS-D was designated NOAA-2 after launch.
**TIROS-M was designated ITOS-1 after launch.
† ITOS-A was designated NOAA-1 after launch.

PRECEDING PAGE BLANK NOT FILMED
PRECEDING PAGE BLANK NOT FILMED

CONTENTS

	Page
INTRODUCTION	1
LAUNCH-ACQUISITION AND ATTITUDE-CONTROL PERFORMANCE OF ITOS-D DYNAMICS SUBSYSTEM	3
ACKNOWLEDGMENTS	5
REFERENCES	6

PRECEDING PAGE BLANK NOT FILMED

ILLUSTRATIONS

Figure		Page
1	Attitude Horizon Sensor Scanning Geometry	14
2	Geometry of the Sun-Synchronous Orbit	15
3	NOAA-2 Dynamics Control Subsystem Element Locations	16
4	Sequence of Events—Attitude Acquisition Showing Dynamics—Control Subsystem Element Locations on the Satellite	17
5	Dynamics-Control Subsystem, Simplified Block Diagram	18
6	Comparison of ITOS-A-C and ITOS-D	19
7	Horizon Sensor Output Processing	20
8	Attitude Telemetry Waveforms	21
9	NOAA-2 Stability Plot	22
10	Nutation Damping	23
11	NOAA-2 SR Attitude Determination Rev 186, 10/30/72, PHI Max 0.216, Lambda 314.986, Gamma 45.94	24
12	Instantaneous Pitch Servo Error Determination, Orbit 253G	25
13	Momentum Control Coil Torquing	26
14-A	NOAA-2 Attitude	27
14-B	NOAA-2 Attitude	28
15	Pitch Attitude Offset versus Wheel Speed Fine-Gain Operation	29
16	NOAA-2 Free Drift Test (Orbits 15 to 30)	30
17	Interface Wiring and Separation Switch Functions	31
18	NOAA-2 Real-Time Beacon Telemetry Data for Pitch Loop-1 Horizon Sensor and Pitch Index	32
19	NOAA-2 Real-Time Beacon Telemetry Data for Pitch Loop-2 Horizon Sensor and Pitch Index	33
20	NOAA-2 Real-Time Beacon Telemetry Data for Pitch Loop-1 Earth Scan Data	34

ILLUSTRATIONS (continued)

Figure		Page
21	NOAA-2 Real-Time Beacon Telemetry Data for Pitch Loop-2 Earth Scan Data	35
22	NOAA-2 Channels 96 and 98 Pitch Loops-1 and -2 Motor Voltage Housekeeping Telemetry TEC/GSFC, Nov. 3, 1972	36
23	NOAA-2 Channels 95 and 97 Pitch Loops-1 and -2 Motor Current Housekeeping Telemetry TEC/GSFC, Nov. 3, 1972	37

TABLES

Table		Page
1	Orbital Elements for NOAA-2	7
2	NOAA-2 Attitude Performance Values	8
3	NOAA-2 Attitude Command History	12

IN-ORBIT PERFORMANCE OF THE ITOS IMPROVED ATTITUDE CONTROL SYSTEM WITH HALL GENERATOR BRUSHLESS MOTOR AND EARTH-SPLITTING TECHNIQUE

INTRODUCTION

NOAA-2, using the improved attitude control system, was launched for the first time on an improved Delta 0300 launch vehicle. Instead of six solid motors, three were used, and the Western Electric Company guidance system was replaced by a new Delta inertial guidance system (DIGS). The specific impulse of the Delta second stage has been improved by using Aerozine 50 and N_2O_4 instead of unsymmetrical dimethyl hydrazine (UDMH) and inhibited red-fuming nitric acid (IRFNA).

The NOAA-2 spacecraft was the first of a new series of meteorological spacecraft which is now providing temperature soundings of the earth's atmosphere as well as direct readout and global cloudcover data. These spacecraft have redundant very high resolution radiometers (VHRR's), vertical temperature profile radiometers (VTPR's), scanning radiometers (SR's), and a single solar proton monitor (SPM) as a secondary sensor. The NOAA-2, weighing 749 pounds (340 kg), was launched from the Air Force Western Test Range (AFWTR) at Vandenberg Air Force Base, California, on October 15, 1972 and has successfully provided high-quality daytime and nighttime pictures of the earth, sea, and cloudtops. On orbit 303, November 8, 1972, NASA turned over control of NOAA-2 to the National Oceanic and Atmospheric Administration (NOAA).

Figure 1 shows the attitude horizon sensor scanning geometry and primary axes of the satellite. Figure 2 shows the geometry of the sun-synchronous orbit. A list of the nominal orbital parameters, before launch on October 15, 1972, and on October 18, 1972, are listed in Table 1.

Figure 3 shows the approximate location of elements of the dynamics subsystem for NOAA-2, and Figure 4 shows the sequence of events during attitude acquisition. Figure 5 is a simplified block diagram of the dynamics subsystem. Figure 6 shows a comparison of the ITOS-A-C and ITOS-D spacecraft. The elements of the dynamics subsystem consist of:

- Redundant nutation dampers
- Redundant momentum-control coils (MCC)
- Functionally redundant roll/yaw-axis control by the quarter-orbit magnetic attitude-control (QOMAC) coil

- Magnetic-bias control (MBC) coil
- Nonredundant digital solar aspect sensor (DSAS)
- Redundant pitch-control electronics (PCE)
- Momentum-wheel assembly (MWA) with redundant motors on the same shaft, redundant satellite earth-facing side reference magnetic pickup (MPU) generators, and redundant CO_2 horizon sensors.

With the exception of the horizon sensors, the magnetic pickups, brushless motor, and the earth-splitting technique, the elements of the dynamics subsystem are described in Reference 1. The exceptions are described in Reference 2. A general description of the entire ITOS-1 and NOAA-1 dynamics and other subsystems can be found in Reference 3. Reference 2 is applicable to NOAA-2 and describes the CO_2 sensors, earth-splitting technique, magnetic pickups, and the brushless motor.

A summary of the highlights of Reference 2 is included at this point to give a better understanding of the control subsystem, blanking, earth-splitting, pitch-attitude control, and attitude telemetry available for control subsystem performance evaluation.

As a result of the dynamic response of the earth sensing system which generates sky-earth (S/E) and earth-sky (E/S) pulses, overshoots may occur giving false indications of the S/E and E/S signals. To ensure against this, blanking is synchronized with each wheel spin at (S/E) thresholding by means of a counting scheme referenced to the output from the wheel rotation position indicator which generates 48 pulses per wheel rotation. Blanking follows the S/E threshold pulse for 60 degrees of wheel rotation for negative overshoots which follow S/E pulses, and for 180 degrees of wheel rotation for positive overshoots which follow E/S pulses (Figures 7, 8, 18, and 19). Each pulse from the encoder represents 7.5 degrees of wheel rotation.

Horizon splitting employs two binary counters of equal capacity to generate a pulse midway between the leading edges of the threshold S/E and E/S horizon pulses. The clock source used to drive the counters is an LC oscillator, which produces pulses at rates of 309 and 618 kHz. The leading edge of the S/E pulse initiates counter-1 operation. Concurrent with the S/E leading edge, clock pulses at the 309-kHz rate are gated into the counters as shown in Figure 7.

Counter 1 runs until it fills, at which time it stops and resets itself. The reset occurs during the scan sky time. Counter-2 operation is initiated by the

leading edge of the E/S pulse. Concurrent with the E/S leading edge, clock pulses at the 309-kHz rate are gated into counter 2. The counter runs until the reset of counter 1 occurs, at which time the count is terminated. At this point, the count differential between the counters is equal to the pulse count accumulated by counter 1 during the interval between S/E and E/S pulses, that is, the earth-scan period (Ref. 4).

The leading edge of the following S/E pulse reinitiates counter-2 operation. Concurrent with this leading edge, clock pulses at the 618-kHz rate are gated into the counter. Counter 2 fills in a period equal to half the time interval between S/E and E/S pulses, as derived during the previous earth scan. At this point, the horizon-splitting pulse is generated. Counter 2 continues to run for a period approximating 6.6 milliseconds, at which time it stops and resets itself. Concurrent with the resetting of counter 2, the horizon-splitting pulse is terminated. The splitting pulse thus derived is of suitable width for utilization in the error detection circuit (Ref. 4). The time occurrence of the earth-splitting pulse (ESP) is compared with the time occurrence of the satellite earth-facing side reference pulse called a pitch-index pulse (PIP). If the PIP occurs before the ESP motor current decreases, the wheel speed decreases and momentum is transferred from the wheel to the satellite to correct the error The opposite is true if the PIP lags the ESP. Figure 8 shows the attitude telemetry waveforms. Only one of these waveforms can be telemetered at any given time. The first and second waveforms are similar to those provided in the TIROS-M and ITOS-A control subsystems. Roll/yaw attitude can be reduced from these waveforms in precisely the same manner as that utilized for TIROS-M and ITOS-A.

Pitch attitude information can be reduced from the second waveform by determining the midpoint of the earth scan and comparing its phasing with the leading edge of the telemetered pitch-index pulse. For the purpose of this computation, the time interval between the 1/2 amplitude points on the leading edges of the S/E and E/S pulses is defined as the earth scan time.

The third waveform permits determination of the sensed attitude error interpreted by the pitch servo. The phasing between the index and threshold horizon pulses shown in Figure 8 is approximate for a local vertical oriented satellite and a nominal momentum condition.

LAUNCH-ACQUISITION AND ATTITUDE-CONTROL PERFORMANCE OF ITOS-D DYNAMICS SUBSYSTEM

The performance of the Delta was within predictions and was essentially as shown in Figure 4. Satellite spinup by the Delta was 2.7 rpm which was in the

expected range of 2.36 to 2.88 rpm. Table 2 lists the predicted and actual satellite performance values. Figure 9 is an NOAA-2 stability plot using inertia values calculated before launch. After clockwise spinup, as viewed from the Delta engine section, separation was commanded by the Delta timer. After separation, the wheel came up to 118 rpm transferring momentum from the satellite to the wheel. As a result, the satellite spin rate decreased to 0.68 rpm about the satellite's pitch axis. With one cycle of high QOMAC on orbit 5, the pitch axis was torqued to be nearly normal to the orbit plane. With the satellite pitch axis normal to the orbit plane and the satellite spin rate at <0.1 rpm (as shown by the intersection of the 150-rpm line in Figure 9), and with solar panels open, the pitch-loop lock-on was commanded. The command to lock on was sent from the Gilmore CDA station on orbit 7 and lock-on occurred in approximately 180 seconds. The MCC was not required to change satellite system momentum before lock-on because the Delta imparted desirable momentum to the satellite during spinup.

Due to a longer-than-expected nutation damper time constant, and a roll attitude error of about 5.7 degrees on orbit 5, lock-on was commanded on orbit 7 when roll attitude error was about 1.5 degrees and the nutation approximated a 0.97-degree half-cone angle. Except for pitch-loop switching on orbits 200 and 225, nutation has been too low to measure since orbit 20. In the closed-loop mode, since orbit 7, the pitch loop contributes to nutation damping due to roll/pitch cross coupling as a result of incorporation of the earth-splitting technique.

The expected nutation damper time constant with the wheel at 115 rpm and solar panels closed was about 84 minutes. The measured value was about 190 to 417 minutes. The expected time constant at lock-on with the pitch loop contributing to damping was about 47 minutes. The measured value was about 65 minutes. Considering the damper time constant, without pitch-loop damping, the value was expected to be about 148 minutes. The value measured was 1287 minutes. The damper performance, during magnetic torquing of the QOMAC and MBC, partly accounts for the delay in achieving the desired attitude for orbit-5 lock-on. The Delta maneuver to place the NOAA-2 pitch axis about 10 degrees from orbit normal was as expected. However, at spacecraft separation, the spacecraft beacon data revealed a half-cone nutation angle of about 7 degrees. Data sampling at a time when the NOAA-2 pitch axis and mutation angle were added made the NOAA-2 pitch axis appear to be about 17 degrees from orbit normal. The reason for the longer than-expected nutation damper time constant has been attributed to possible leaky nutation dampers by RCA/AED, as a result of extensive damper testing. Special measures will be made to ensure that future ITOS dampers contain sufficient oil.

Another contribution to the delay to lock on was the requirement to correct for an unexpected residual dipole along the satellite's Z axis. Testing prior to launch revealed a -0.02 ATM^2 dipole. The value measured during free drift tests in orbit revealed a -2 ATM^2 residual dipole. The dipole could have been the result of magnetic dipole testing errors, exposing the satellite too closely to the OSCAR* 50 ATM^2 magnet or some unknown field. Precautions to prevent the above will be taken on future ITOS.

Another item of interest which did not operate as expected, but does not prevent satisfactory in-orbit performance, is the fact that the wheel speed set point for 115 and 150-rpm operation in orbit was inadvertently set about 2 rpm high. Therefore, the center of the chart in Figure 15 was changed to 152 rpm.

Figures 9 to 23, Tables 2 and 3, and the following references describe the NOAA-2 control subsystem performance in orbit.

ACKNOWLEDGMENTS

The author wishes to acknowledge the efforts of the following RCA/AED personnel for their contributions to this document.

Joe Elko
Lou Muhlfelder
Roger Hogan
Tom Ferria

*A secondary payload with a bar permanent magnet.

REFERENCES

1. William M. Peacock. "Attitude Control Performance of the Improved Television Infrared Observation Satellite (ITOS-1)." NASA/GSFC X-481-71-108. March 1971.

2. William M. Peacock. "Improved ITOS Attitude Control System With Hall Generator Brushless Motor and Earth-Splitting Technique." NASA/GSFC X-480-71-404. August 1971.

3. ITOS Night-Day Meteorological Satellite. The document is available from Superintendent of Documents, U.S. Government Printing Office, Washington, D.C. 20402.

4. ITOS-B Spacecraft Final Engineering Report. RCA/AED R 3735 F. NAS5-10306, December 28, 1971.

5. John McCloskey. NOAA-2 Final Report of Attitude Results. December 16, 1972.
   ITOS Ground Station at GSFC.

Table 1

Orbital Elements for NOAA-2

Orbital Elements	Predicted October 15, 1972	Actual October 18, 1972
Semimajor axis	7839.845 km	7829.204 km
Eccentricity	0.000257	0.000375
Inclination	101.76°	101.77°
Mean anomaly	265.920°	124.774°
Argument of perigee	78.401°	235.486°
Motion minus	1.9168°/day	1.9251°/day
Right ascension of ascending node	330.585°	340.700°
Motion plus	0.9862°/day	0.9918°/day
Anomalistic period	115.1 min	114.9 min
Height of perigee	1460 km	1448.1 km
Height of apogee	1464 km	1453.98 km
Velocity at perigee	25676 km/hr	25697 km/hr
Velocity at apogee	25663 km/hr	25677 km/hr
Geocentric latitude of perigee	73.539°	53.77°

Table 2

NOAA-2 Attitude Performance Values

Event or Measurement	Predicted Value	Actual Value
1. Satellite body rate at separation with solar panels closed	2.62 rpm	2.7 rpm (see Figure 9)
2. Satellite body rate with wheel speed at 118 rpm with solar panels closed*	0.61 rpm	0.68 rpm (see Figure 9)
3. Satellite pitch axis degrees away from normal to orbit plane at separation from the Delta	$10 \pm 2^\circ$	$\simeq 17^\circ$†
4. Satellite body rate with wheel speed at 152 rpm with solar panels open*	$\simeq 0.25$ rpm	<0.1 rpm
5. Satellite body rate when the command to close the pitch loop was sent	$\simeq 1$ rev/orbit	$\simeq 1$ rev/orbit
6. Time to lock on earth after the command to close the pitch loop	<6 min	$\simeq 180$ sec
7. Satellite aligns and maintains attitude about the pitch axis	$\pm 1^\circ$	$<0.5^\circ$ (see Figure 11)
8. Pitch servo error	$\pm 1^\circ$	$<0.5^\circ$ (see Figure 12)
9. Pitch jitter	$\simeq 0.05^\circ$/sec sec	$\simeq < 0.05^\circ$/sec
Roll jitter	$\simeq 0.05^\circ$/sec	$\simeq < 0.05^\circ$/sec
10. Maximum half-cone angle at separation and nutation period	$<13^\circ$ half-cone angle Period 37 s	$\simeq 7^\circ$ half-cone angle 24.7 s
11. Frequency of MCC torquing to maintain 151 to 154 rpm**	$\simeq 30$ orbits or daily as required	Daily (see Figure 13)
12. High-torque QOMAC performance	$\simeq 10^\circ$/orbit	See Table 3
13. Frequency and rate of torquing high QOMAC (see Table 3)	Acquisition only	See Table 3
14. Low-torque QOMAC performance	$\simeq 1.2^\circ$/orbit	See Table 3

*Bias setting for wheel speed for pitch loops 1 and 2 for ITOS-D was for a wheel speed of about 152 rpm. Also, the wheel speed was about the same rpm above 115 rpm. See Figure 15.

†Includes spacecraft nutation of about a 7-degree half-cone angle. The Delta yaw maneuver was as predicted. See Figure 10 for nutation of pitch axis about the momentum vector.

**Bias setting of wheel speed for pitch loops 1 and 2 for ITOS-D was for a wheel speed of about 152 rpm. See figure 15.

B

Table 2 (Continued)

NOAA-2 Attitude Performance Values

Event or Measurement	Predicted Value	Actual Value
15. Frequency and rate of torquing low QOMAC as required	≃1.2°/orbit	See Table 3
16. MBC performance with switch positions checked	0.36 to 3.6°/day 0.36° granularity	See Table 3
17. Frequency and rate of torquing MBC	≃Weekly change: use is continuous	MBS position No. 10 positive (see Table 3)*
18. MBC performance as backup for QOMAC	≃0.36 to 4.1°/day 0.36° granularity MBS Position 1 to 10 (0.1 to 1.0 ATM^2)	Orbits 14 and 52 (see Table 3)
19. Unipolar torque performance	0.64 to 4.1°/day 0.64° granularity	Use continually (see Table 3)
20. Frequency and rate of torquing of unipolar torque	Use continuously and change weekly	See Table 3
21. Permanent magnet with N-S pole along spin axis for magnetic bias effect†	-0.02 ATM^2	-2 ATM^2 (see Figure 16)
22. Pitch-loop 1		See Table 2 note for events 2, 4, and 11
Open-loop coarse	115 rpm	
Open-loop normal	150 rpm	
Closed-loop fine	150 rpm	
Closed-loop coarse	150 rpm	
Emergency mode	≃500 rpm	
23. Pitch-loop 2		Same as event 22
Open-loop coarse	115 rpm	
Open-loop normal	150 rpm	
Closed-loop fine	150 rpm	
Closed-loop coarse	150 rpm	
Emergency mode	≃500 rpm	
24. DSAS (use only in acquisition mode)	Provide sun angle and S/C body rate	Readings are good

*See Table 3 showing magnetic torquing. Also see polar plot in Figures 14 A and B which show drift and torquing.

†No magnet installed on ITOS-D. Magnetic dipole test results indicated that a magnet would not be needed. The measured residual dipole in orbit was -2 ATM^2 along the pitch (-Z) axis of the spacecraft.

Table 2 (Continued)

NOAA-2 Attitude Performance Values

Event or Measurement	Predicted Value	Actual Value
25. Separation switches provide pitch-loop motor power at separation from Delta. Also arms solar panel relay for solar array deployment so command from CDA station during orbit 5 will deploy panels. One separation switch removes VTPR caging at separation. There are three separation switches.	Provide power to selected pitch-loop motor at separation, arm for solar panel deployment and provide VTPR caging during ascent until S/C separation	Operated properly (see Figure 17)
26. Horizon sensor 1 analog on beacon Sample of horizon sensor and index pulses. See Figure 18.	Bias level: -2.5 v ±10 percent Peak pulse +2.0 v +0.0 v - 0.25 v referenced to bias for radiance difference of 6.3 $\times 10^{-4}$ watts/con^2-str	Data are good See Figure 18
27. Horizon sensor 2 analog on beacon	Same as event 26	Data are good (see Figure 19)
28. Earth-splitting pulse pitch-loop 1	Not telemetered	
29. Earth-splitting pulse pitch-loop 2	Same as event 28	
30. Magnetic pick-up pitch-loop 1 (PIP)	Bias level: 0 +0.0 v - 0.5 v Peak pulse -15 v ±10 percent pulsewidth 3.5 to 7.7 ms	See Figures 20 and 21
31. Magnetic pick-up pitch-loop 2 (PIP)	Same as event 30	See Figures 20 and 21
32. Earth scan telemetry pitch-loop 1. S/E and E/S and index reference amplitudes and pulsewidth	Bias level: -0.9 ±0.2 v Peak pulse threshold -4.3 ± 10 percent Threshold pulse width 6 to 17 ms for S/E and E/S Index pulsewidth ≃3.5 to 7.7 ms	See Figure 20

Table 2 (Continued)

NOAA-2 Attitude Performance Values

Event or Measurement	Predicted Value	Actual Value
33. Earth-scan telemetry pitch-loop 2 S/E and E/S and index reference	Same as event 32	See Figure 21
34. Motor voltage in normal mission mode of operation 152 rpm closed loop with pitch-loop 1 operating	≃10 v	≃10 v (see Figure 22)
35. Motor voltage in normal mission mode of operation 152 rpm closed loop with pitch-loop 2 operating	≃10 v	≃10 v (see Figure 22)
36. Motor voltage pitch-loop 1 while pitch-loop 2 is operating at 150 rpm (CEMF motor 1)	≃8 v	≃8 v (see Figure 22)
37. CEMF motor 2	≃8 v	≃8 v (see Figure 22)
38. Mission mode motor 1 drive current	≃40 ma	30 to 40 ma (see Figure 23)
39. Mission mode motor 2 drive current	≃40 ma	30 to 40 ma (see Figure 23)
40. Mission mode power to operate motor 1	≃0.4 watt	Dwell 0.3 to 0.49 w (see Figures 22 and 23)
41. Mission mode power to operate motor 2	≃0.4 watt	Dwell 0.3 to 0.49 w (see Figures 22 and 23)
42. Motor-1 torque	<≃6 oz. in	≃3.37 oz. in (see Figures 22 and 23)
43. Motor-2 torque	<≃6 oz. in	≃3.00 oz. in (see Figures 22 and 23)

Table 3

NOAA-2 Attitude Command History*

Rev	Event	Period of Event
002G	3 cycles high torque	56 min 02 s AAN***
005G	1 cycle high torque	48 min 13 s AAN***
013G	1 cycle high torque	13 min 58 s AAN***
014G	2 cycles MBC backup	14 min 28 s AAN***
015G	MBC off	
↓	FREE DRIFT TEST (ORBITS 15 to 30)	See Figure 16
030G	1 cycle high torque	06 min 02 s AAN***
033G	UP** QOMAC 05 min 04 s pulsewidth	56 min 55 s AAN***
↓	MODIFIED DRIFT TEST	
052G	4 cycles MBC backup	14 min 58 s AAN***
054G	MBC off	
055G	MBC step 10 positive UP** QOMAC 06 min 24 s pulsewidth	55 min 12 s AAN***
065G	MBC off 3 cycles low torque	11 min 20 s AAN***
067W	MBC step 10 positive UP** QOMAC 06 min 40 s pulsewidth	58 min 12 s AAN***
077G	MBC off, QOMAC off	
079W	MBC step 10 positive UP** QOMAC 06 min 40 s pulsewidth	57 min 0 s AAN***
089G	MBC off, QOMAC off	
091W	MBC step 10 positive UP** QOMAC 06 min 40 s pulsewidth	56 min 36 s AAN***
102G	MBC off, QOMAC off	
104W	MBC step 10 positive UP** QOMAC 06 min 24 s pulsewidth	56 min 36 s AAN***
117W	MBC off, QOMAC off	
119G	MBC step 10 positive UP** QOMAC 06 min 08 s pulsewidth	56 min 36 s AAN***
136W	UP** QOMAC reset	
144G	UP** QOMAC reset	
150W	2 cycles low torque	32 min 36 s AAN***

* See reference 5.
** Unipolar (UP)
*** After ascending node (AAN)

Table 3 (Continued)

NOAA-2 Attitude Command History

Rev	Event	Period of Event
152G	UP** QOMAC 06 min 08 s pulsewidth	56 min 36 s AAN***
170G	UP** QOMAC reset	
180W	2 cycles low torque	19 min 45 s AAN***
182G	UP** QOMAC 05 min 52 s pulsewidth	56 min 36 s AAN***
194G	UP** QOMAC reset	
206G	2 cycles low torque	27 min 04 s AAN***
208G	UP** QOMAC 05 min 52 s pulsewidth	00 min 00 s AAN***
219G	UP** QOMAC reset	
226G	MBC off	
231G	MBC step 10 positive UP** QOMAC 05 min 26 s pulsewidth	00 min 00 s AAN***
245G	UP** QOMAC reset	
256G	UP** QOMAC 06 min 40 s pulsewidth	00 min 00 s AAN***
265G	MBC off 2 cycles low torque	15 min 33 s AAN***
266G	MBC step 10 positive UP** QOMAC 05 min 36 s pulsewidth	00 min 00 s AAN***
273W	MBC off. QOMAC off	
279G	2 cycles low torque MBS 10 positive	
281G	UP** QOMAC 0.05 min 36 s pulsewidth	00 min 00 s AAN***
302	UP** QOMAC reset	
303	Turned over to NOAA on November 8, 1972	

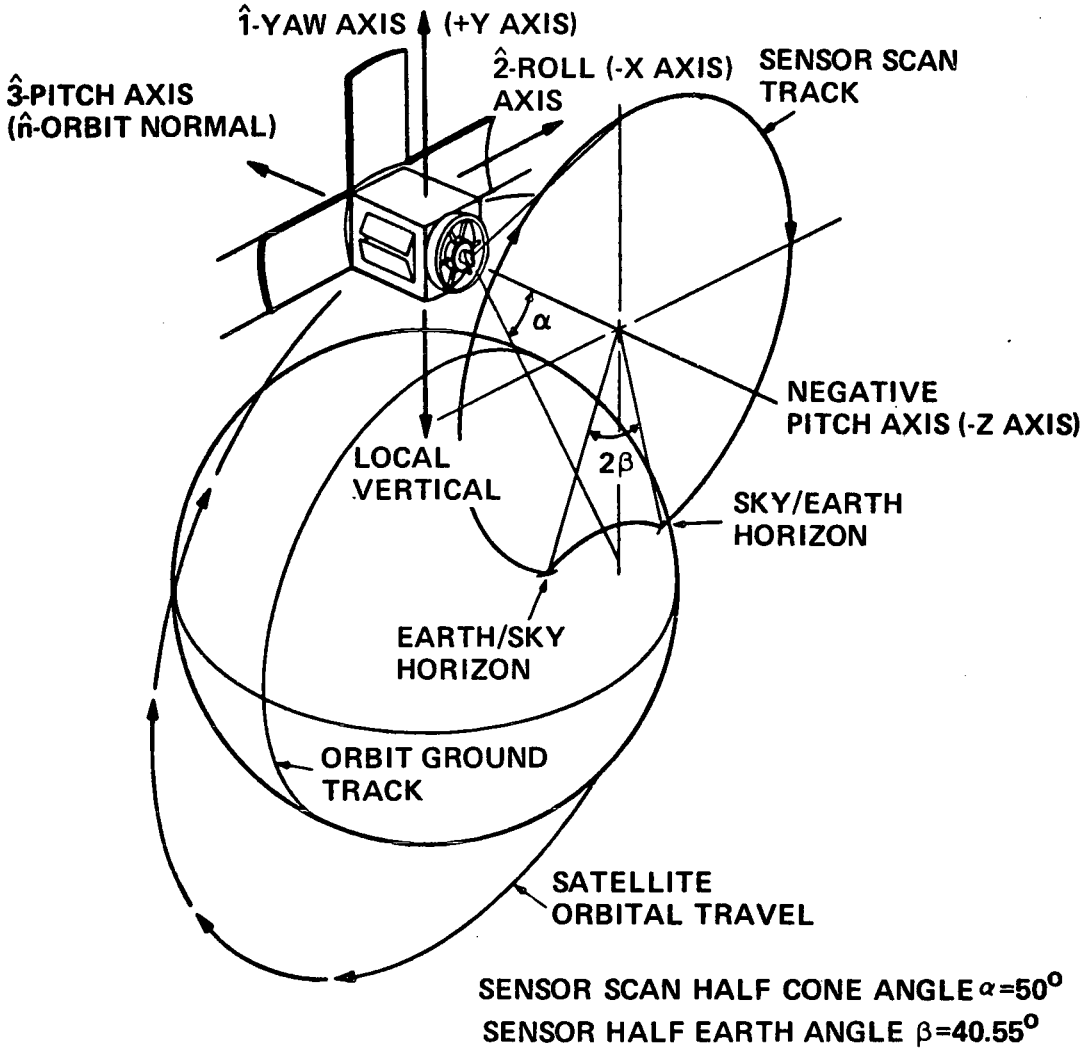

Figure 1. Attitude Horizon Sensor Scanning Geometry

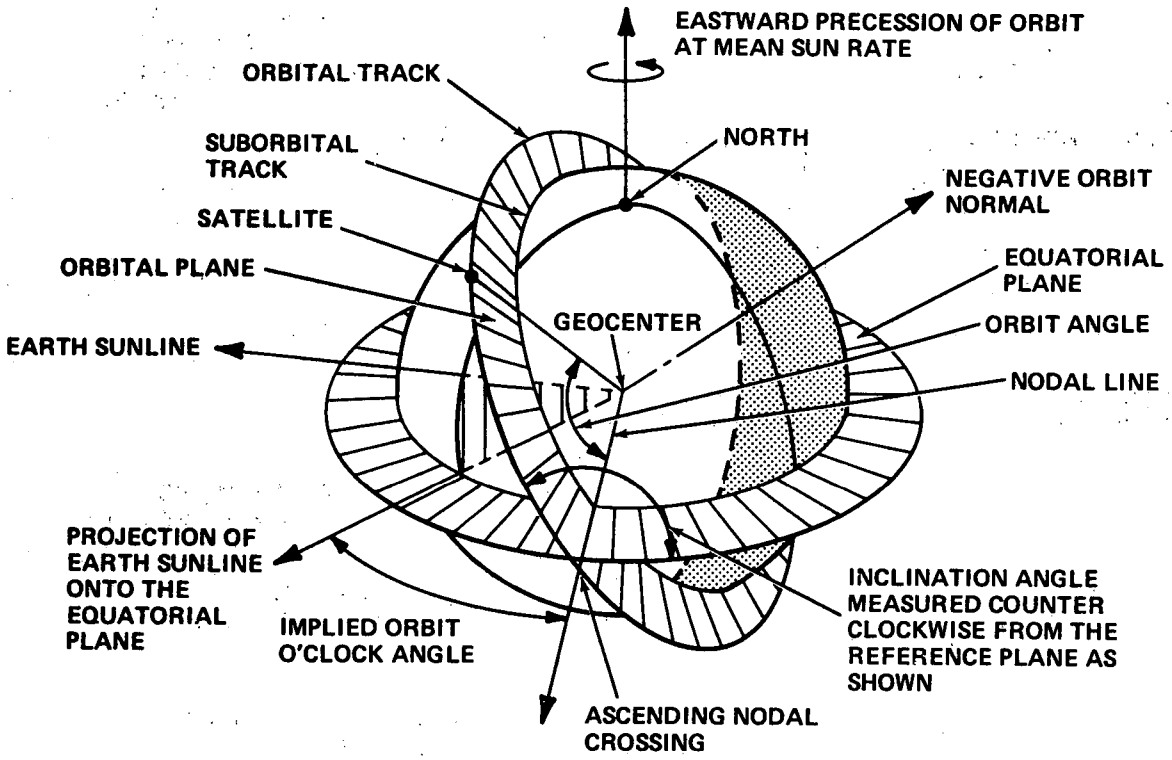

Figure 2. Geometry of the Sun-Synchronous Orbit

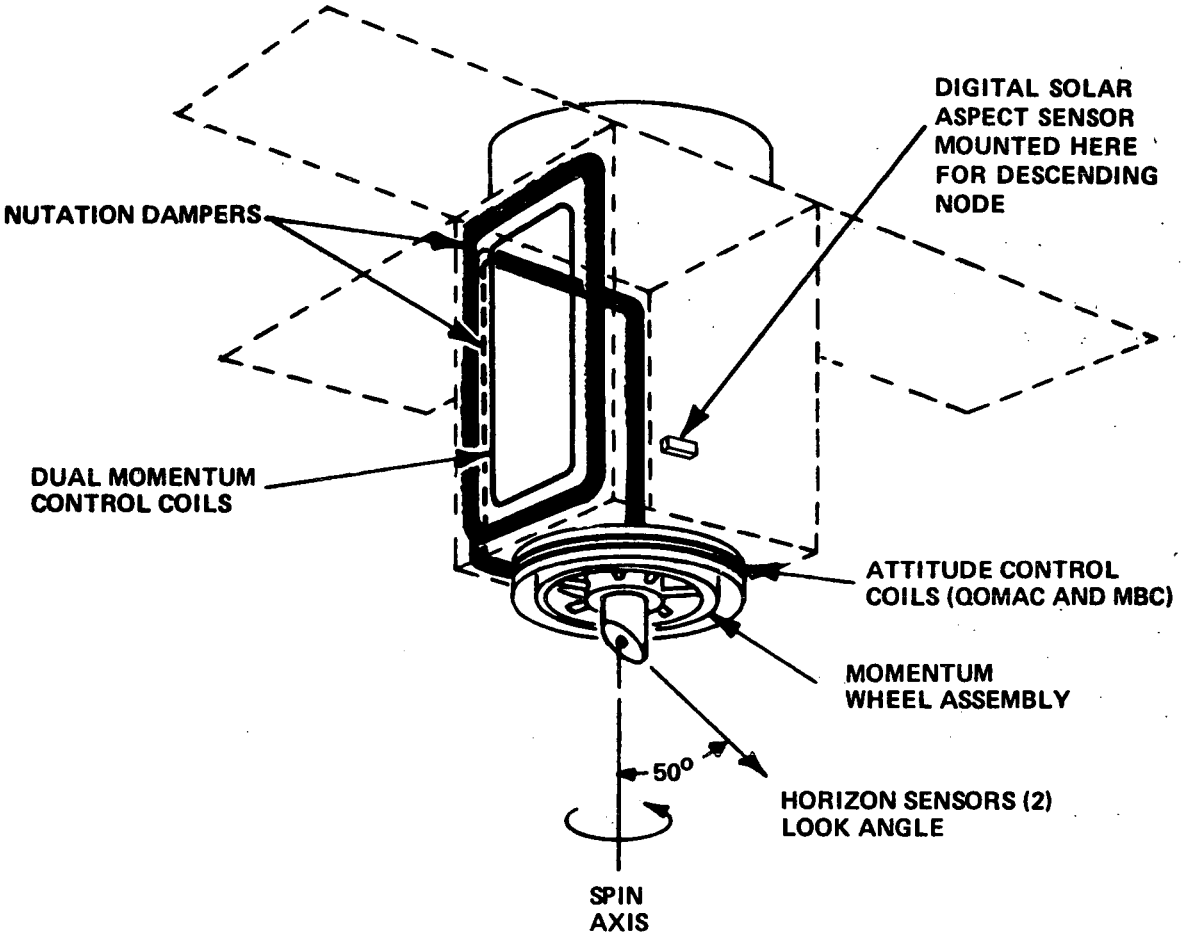

Figure 3. NOAA-2 Dynamics Control Subsystem Element Locations

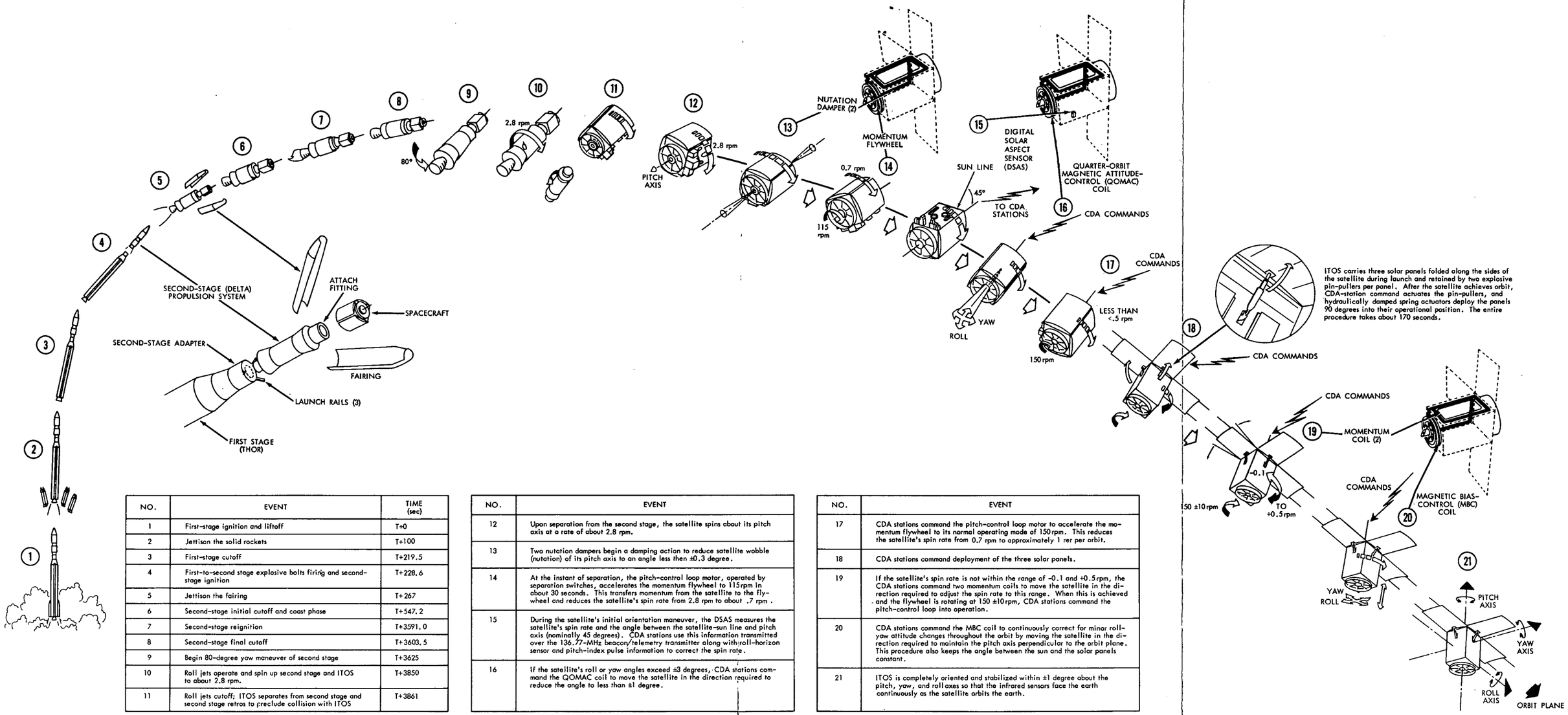

NO.	EVENT	TIME (sec)
1	First-stage ignition and liftoff	T+0
2	Jettison the solid rockets	T+100
3	First-stage cutoff	T+219.5
4	First-to-second stage explosive bolts firing and second-stage ignition	T+228.6
5	Jettison the fairing	T+267
6	Second-stage initial cutoff and coast phase	T+547.2
7	Second-stage reignition	T+3591.0
8	Second-stage final cutoff	T+3603.5
9	Begin 80-degree yaw maneuver of second stage	T+3625
10	Roll jets operate and spin up second stage and ITOS to about 2.8 rpm.	T+3850
11	Roll jets cutoff; ITOS separates from second stage and second stage retros to preclude collision with ITOS	T+3861

NO.	EVENT
12	Upon separation from the second stage, the satellite spins about its pitch axis at a rate of about 2.8 rpm.
13	Two nutation dampers begin a damping action to reduce satellite wobble (nutation) of its pitch axis to an angle less then ±0.3 degree.
14	At the instant of separation, the pitch-control loop motor, operated by separation switches, accelerates the momentum flywheel to 115rpm in about 30 seconds. This transfers momentum from the satellite to the flywheel and reduces the satellite's spin rate from 2.8 rpm to about .7 rpm.
15	During the satellite's initial orientation maneuver, the DSAS measures the satellite's spin rate and the angle between the satellite-sun line and pitch axis (nominally 45 degrees). CDA stations use this information transmitted over the 136.77-MHz beacon/telemetry transmitter along with roll-horizon sensor and pitch-index pulse information to correct the spin rate.
16	If the satellite's roll or yaw angles exceed ±3 degrees, CDA stations command the QOMAC coil to move the satellite in the direction required to reduce the angle to less than ±1 degree.

NO.	EVENT
17	CDA stations command the pitch-control loop motor to accelerate the momentum flywheel to its normal operating mode of 150rpm. This reduces the satellite's spin rate from 0.7 rpm to approximately 1 rer per orbit.
18	CDA stations command deployment of the three solar panels.
19	If the satellite's spin rate is not within the range of -0.1 and +0.5rpm, the CDA stations command two momentum coils to move the satellite in the direction required to adjust the spin rate to this range. When this is achieved and the flywheel is rotating at 150 ±10rpm, CDA stations command the pitch-control loop into operation.
20	CDA stations command the MBC coil to continuously correct for minor roll-yaw attitude changes throughout the orbit by moving the satellite in the direction required to maintain the pitch axis perpendicular to the orbit plane. This procedure also keeps the angle between the sun and the solar panels constant.
21	ITOS is completely oriented and stabilized within ±1 degree about the pitch, yaw, and roll axes so that the infrared sensors face the earth continuously as the satellite orbits the earth.

NOTE: Satellite Sensors and Dynamics Components shown here are for ITOS-D.

Figure 4. Sequence of Events-Attitude Acquisition Showing Dynamics-Control Subsystem Element Locations on the Satellite

FOLDOUT FRAME 1

FOLDOUT FRAME 2

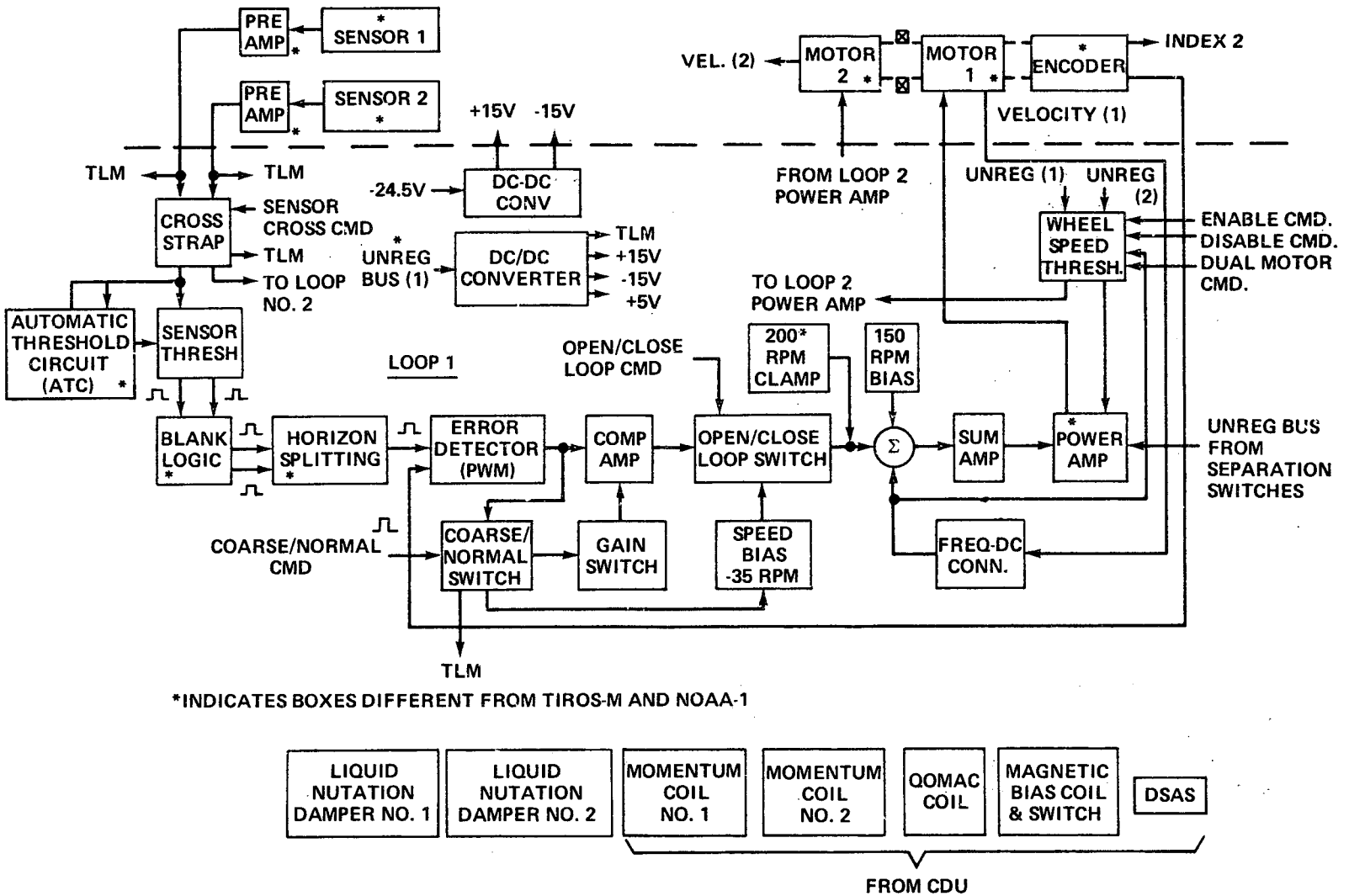

Figure 5. Dynamics Control Subsystem, Simplified Block Diagram

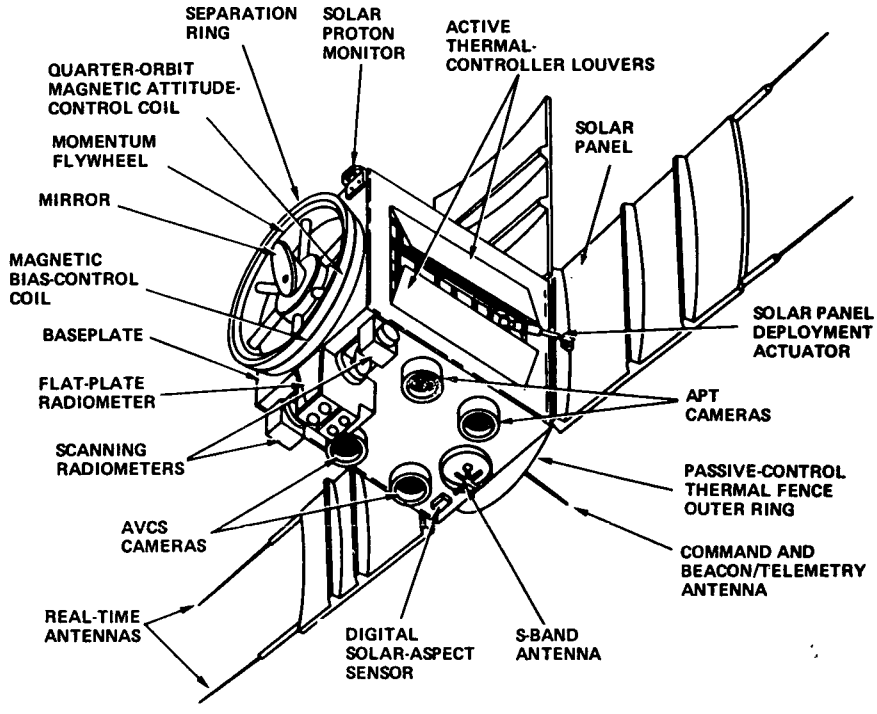

ITOS-A-C Spacecraft

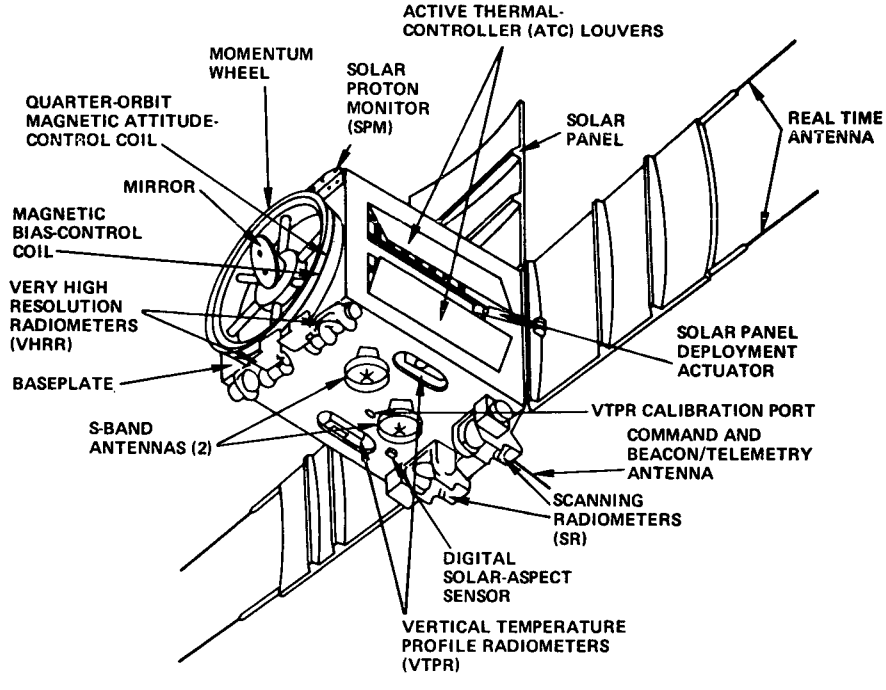

ITOS-D Spacecraft

Figure 6. Comparison of ITOS-A-C and ITOS-D

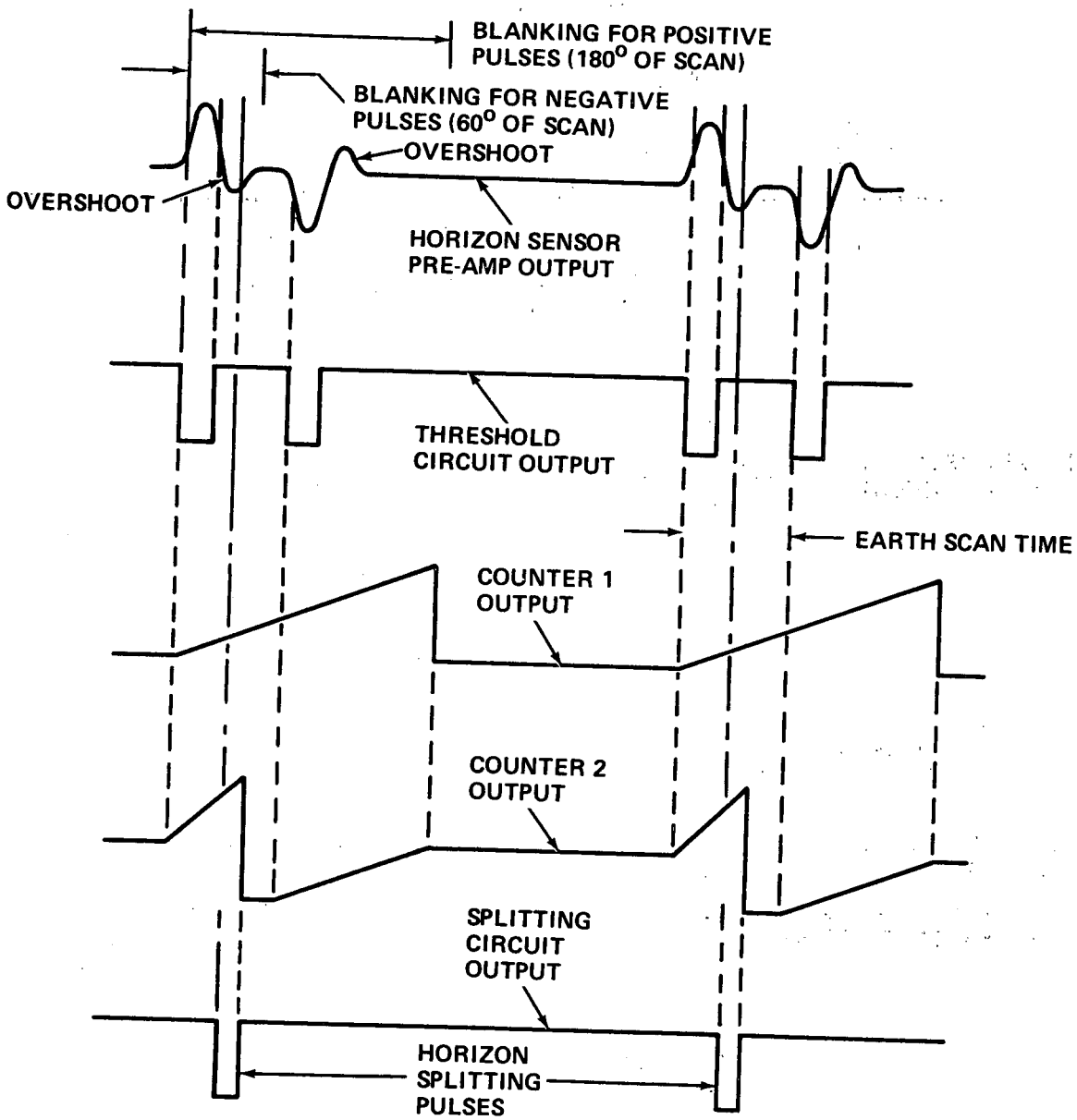

Figure 7. Horizon Sensor Output Processing

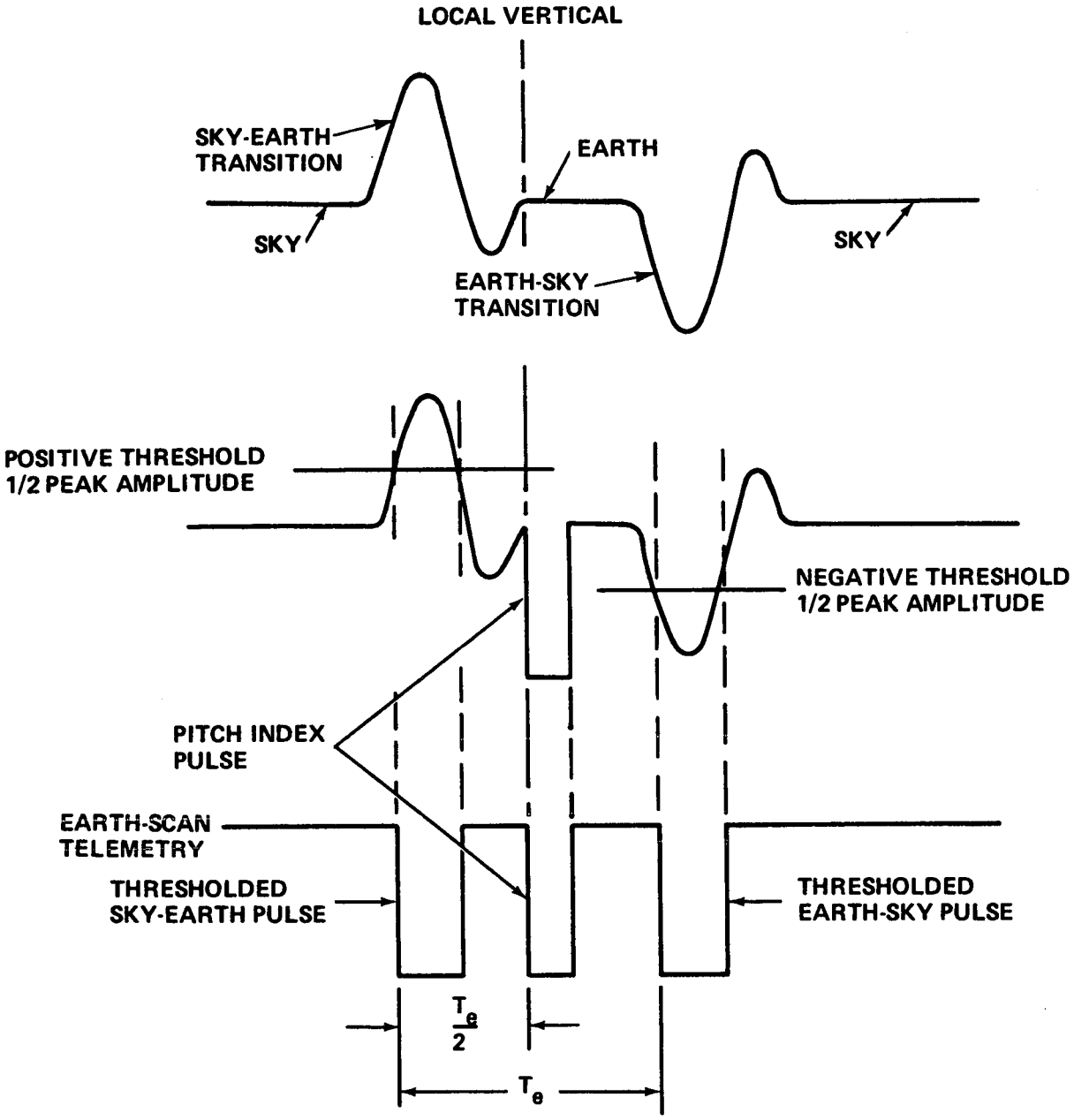

Figure 8. Attitude Telemetry Waveforms

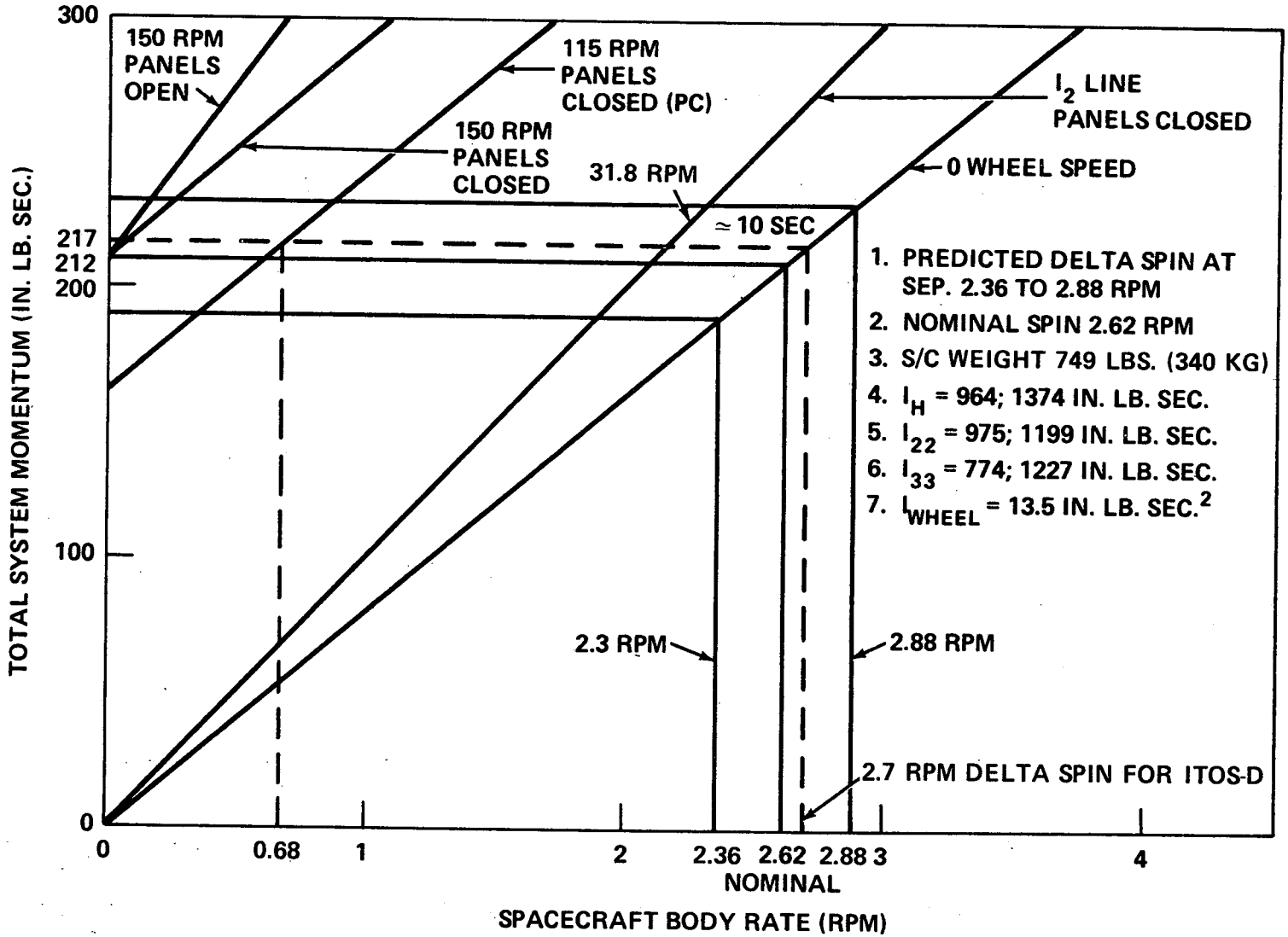

Figure 9. ITOS-D Stability Plot

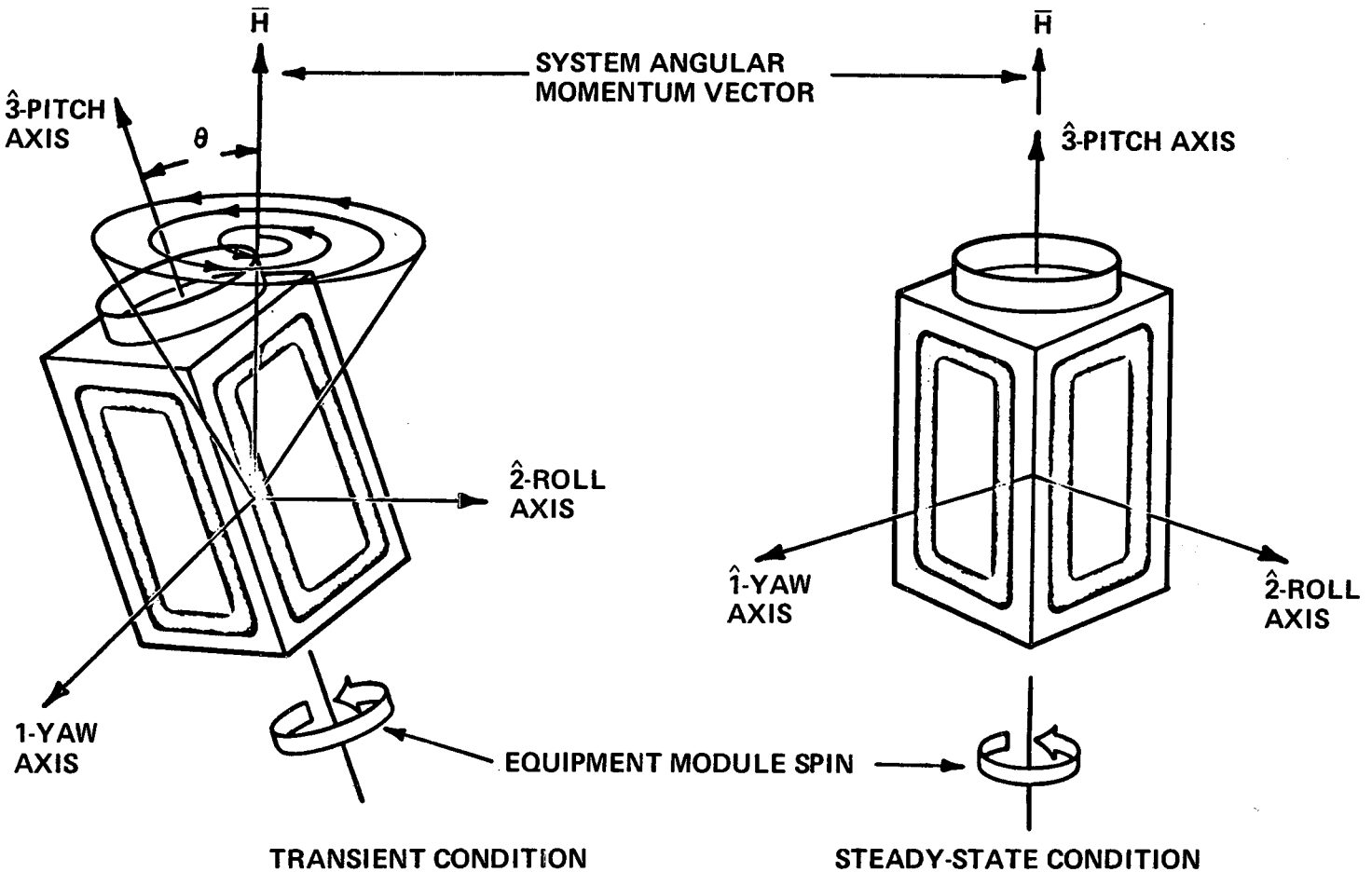

Figure 10. Nutation Damping

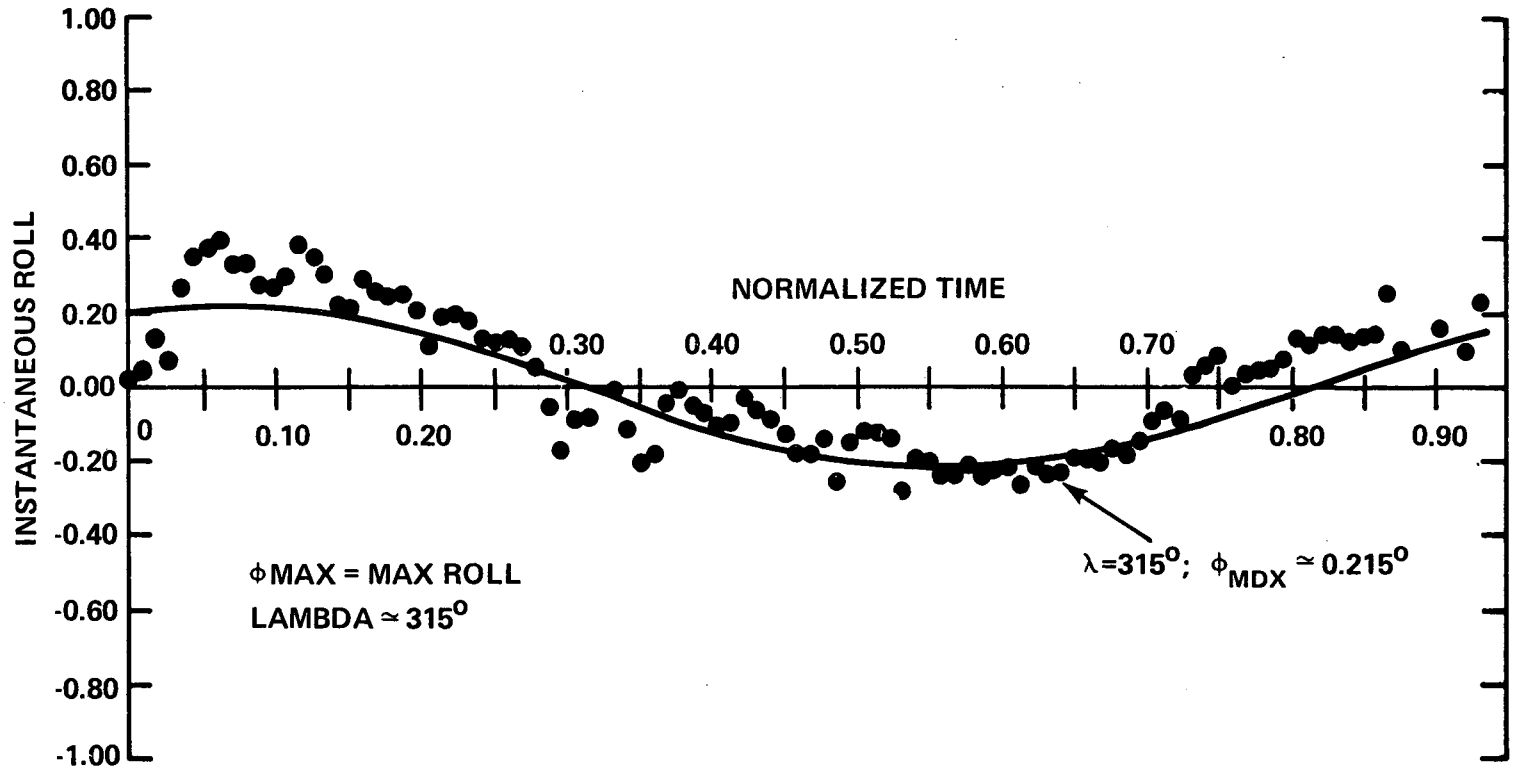

Figure 11. NOAA-2 SR Attitude Determination Rev 186, 10/30/72, PHI Max 0.216
Lambda 314.986, Gamma 45.94

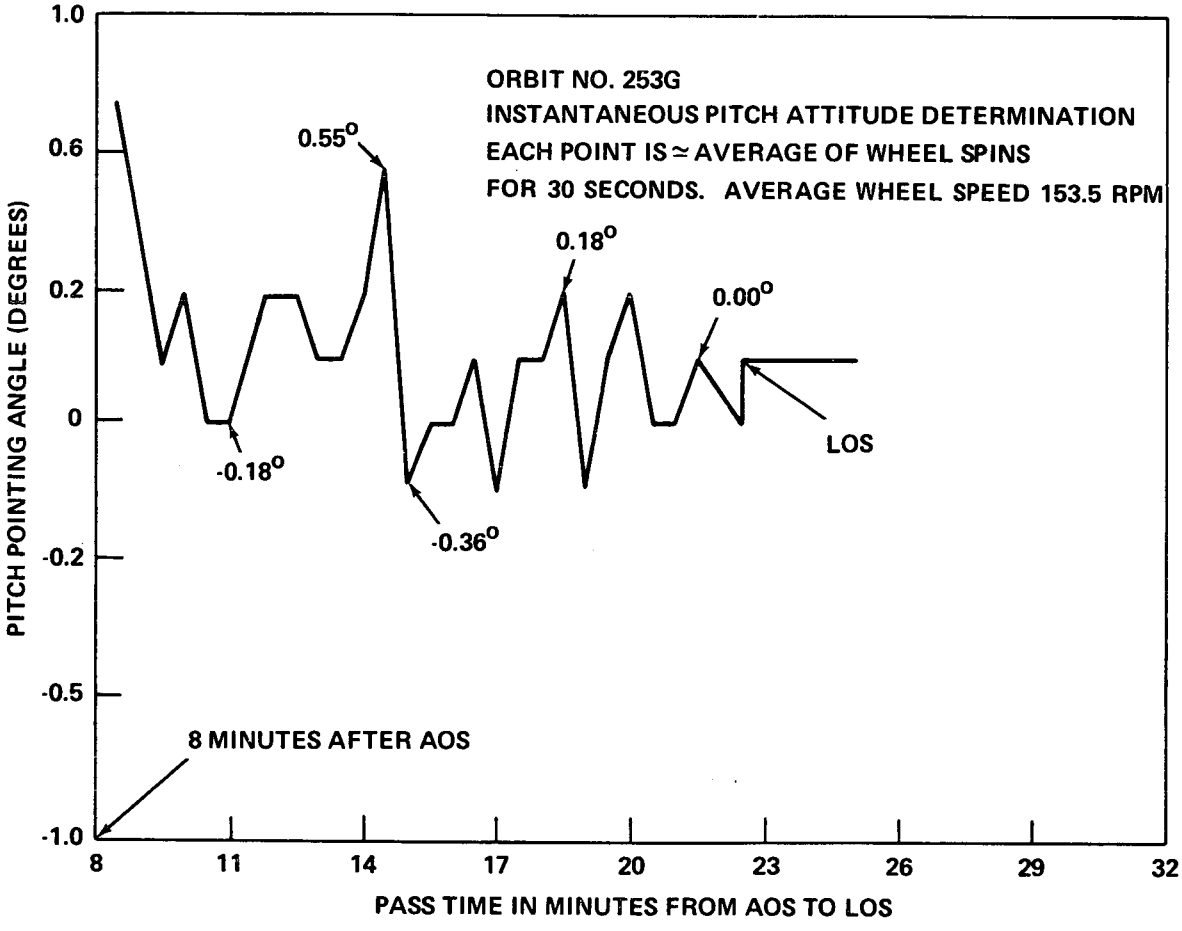

Figure 12. Instantaneous Pitch Servo Error Determination, Orbit 253G

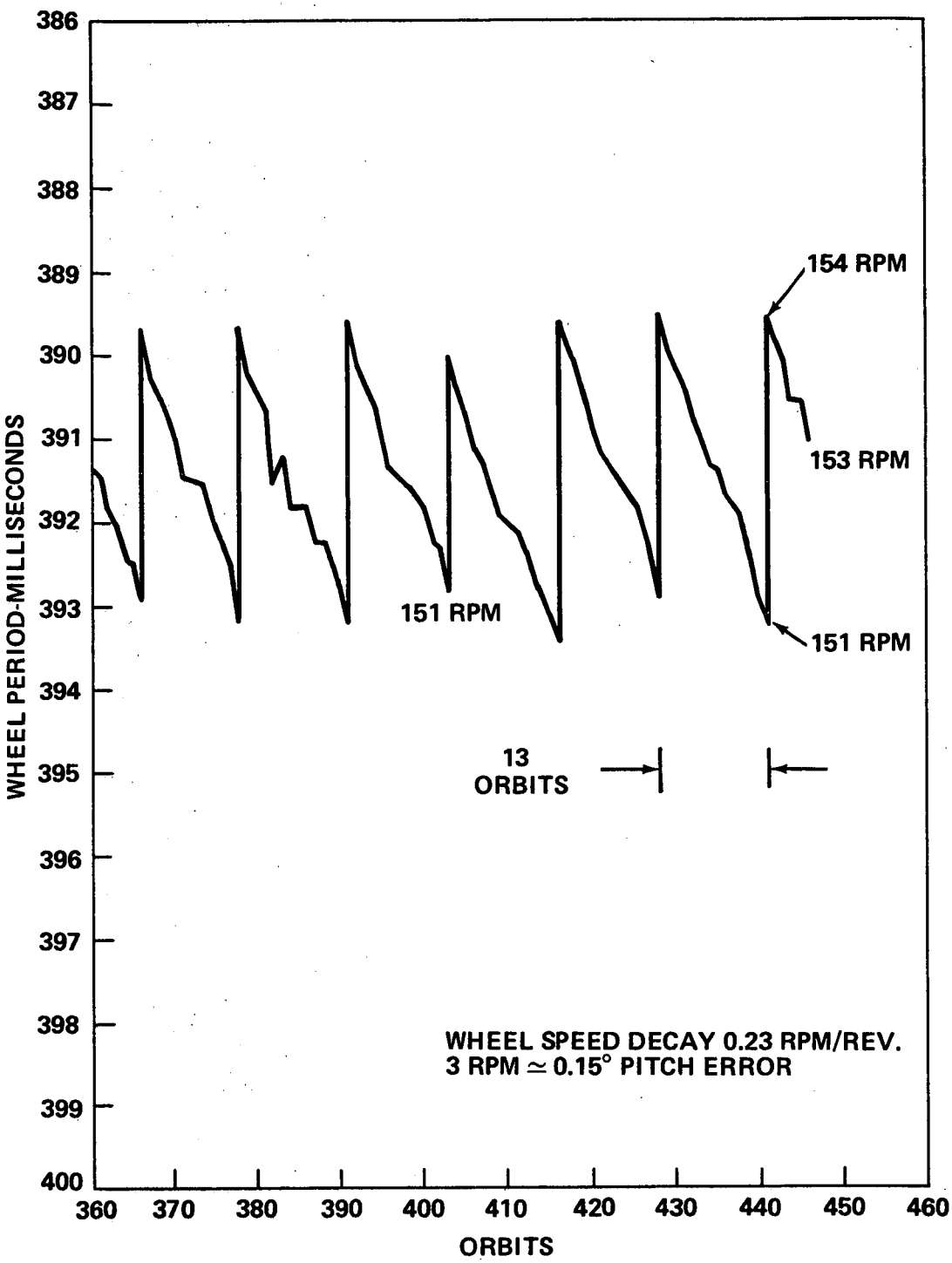

Figure 13. Momentum Control Coil Torquing

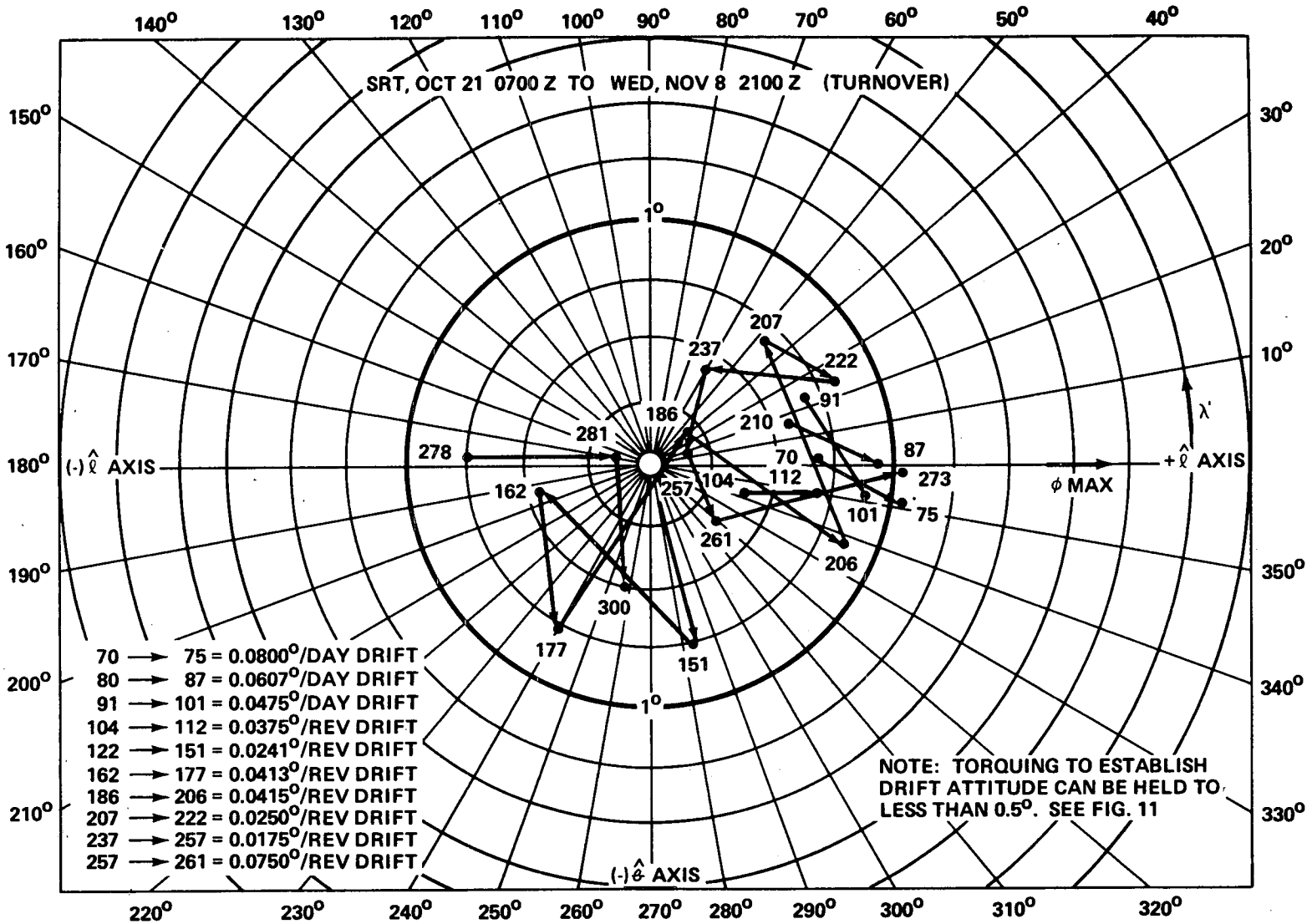

Figure 14-A. NOAA-2 Attitude

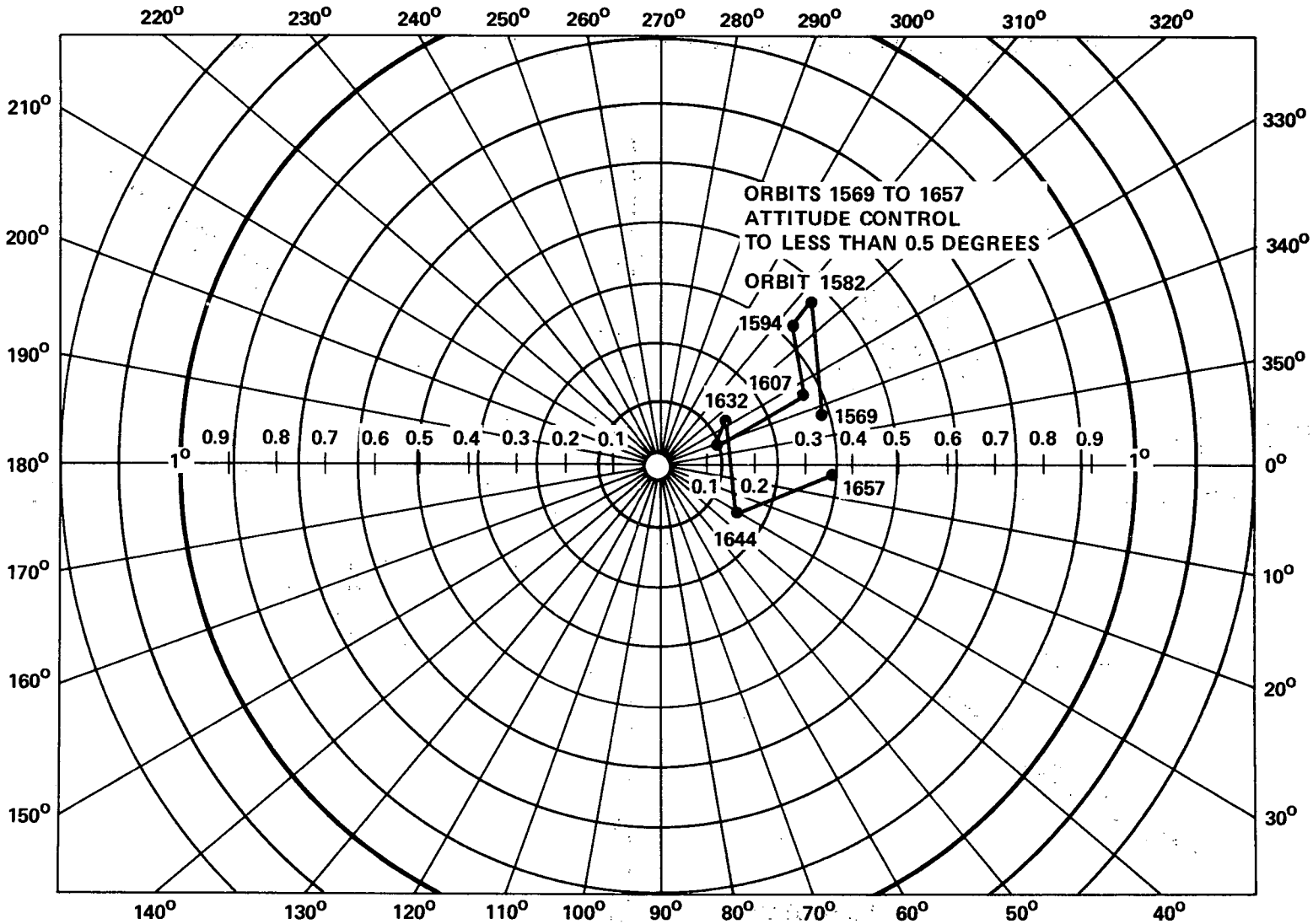

Figure 14-B. NOAA-2 Attitude

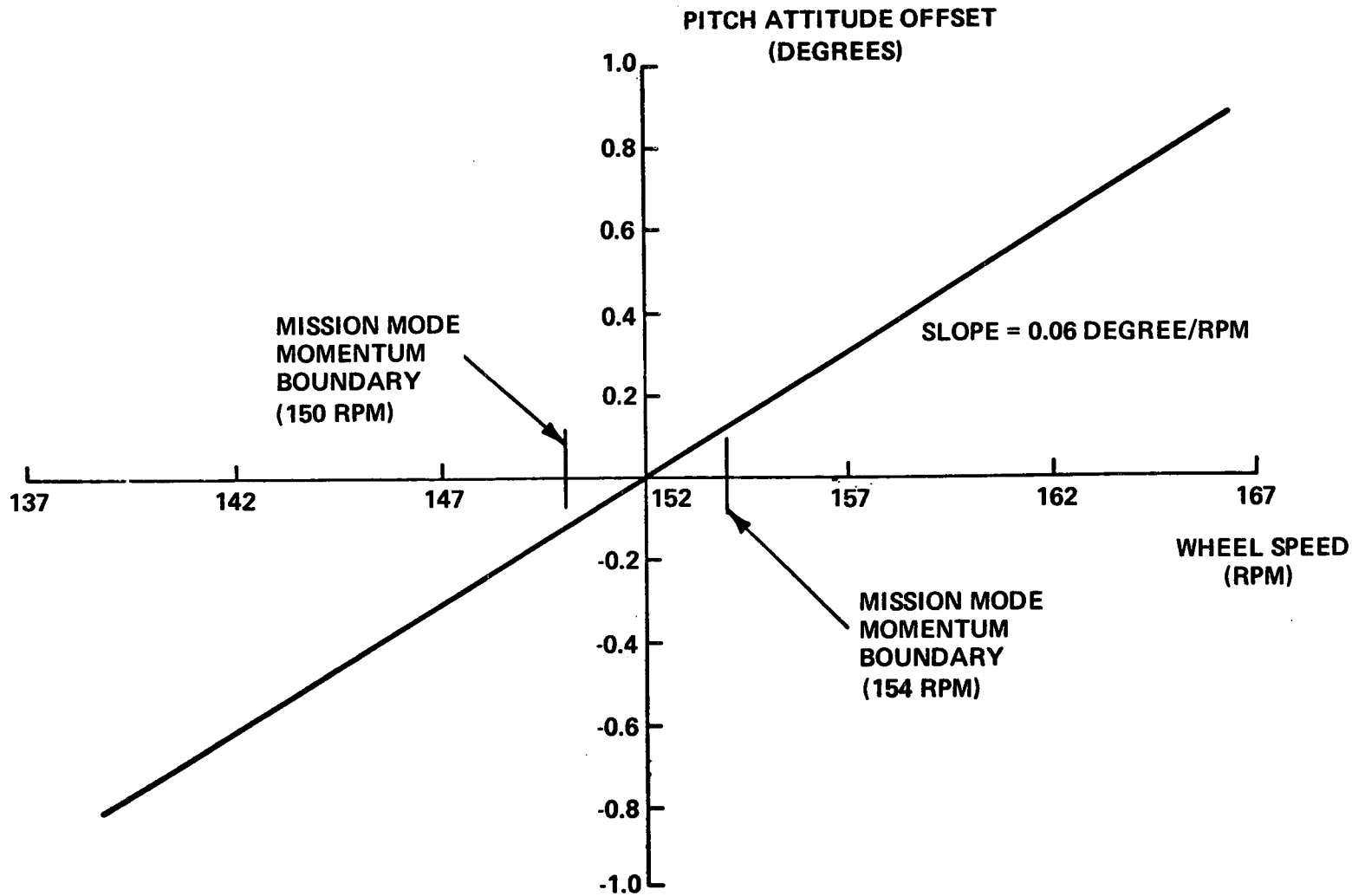

Figure 15. Pitch Attitude Offset versus Wheel Speed Fine-Gain Operation

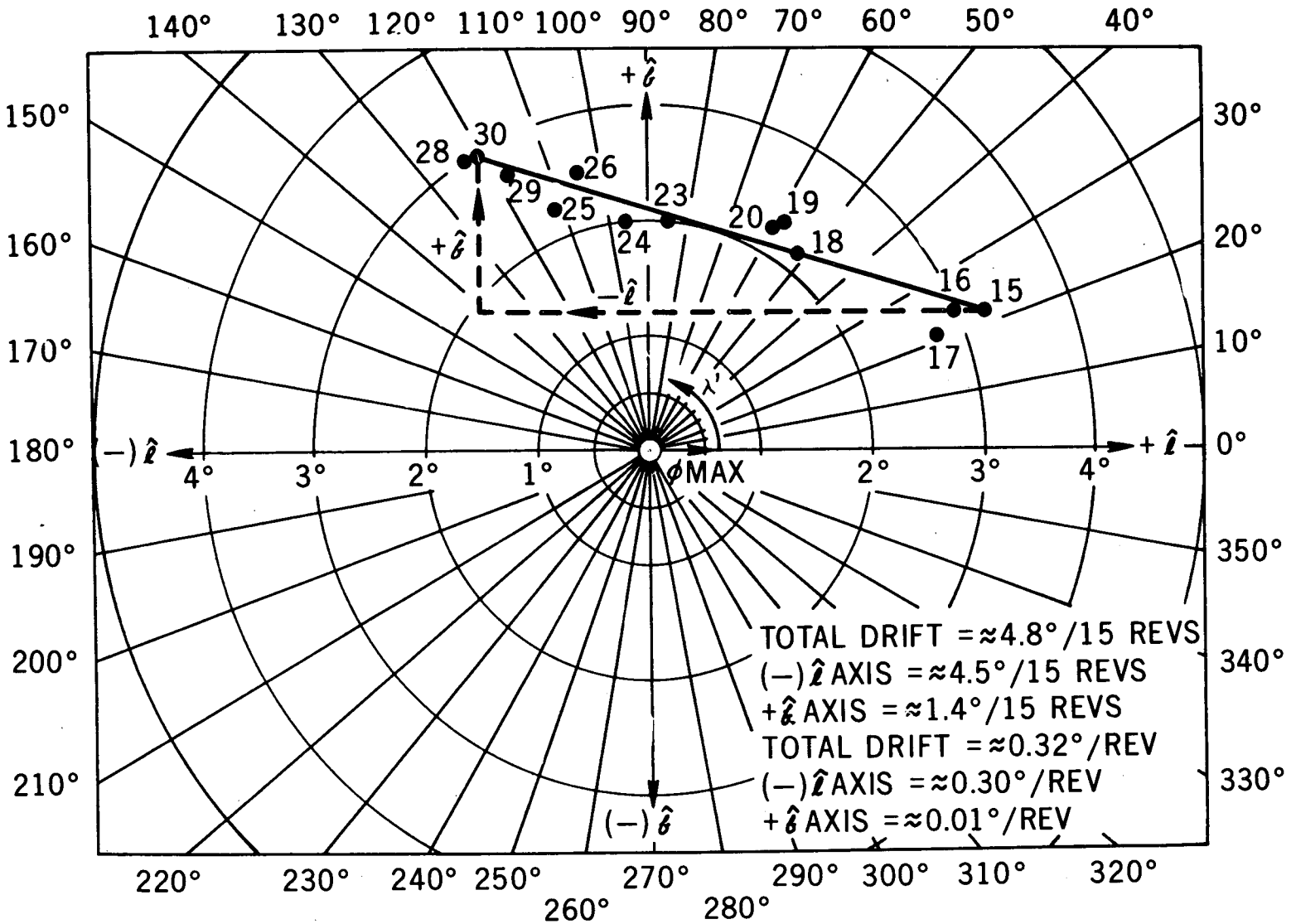

Figure 16. NOAA-2 Free Drift Test (Orbits 15 to 30)

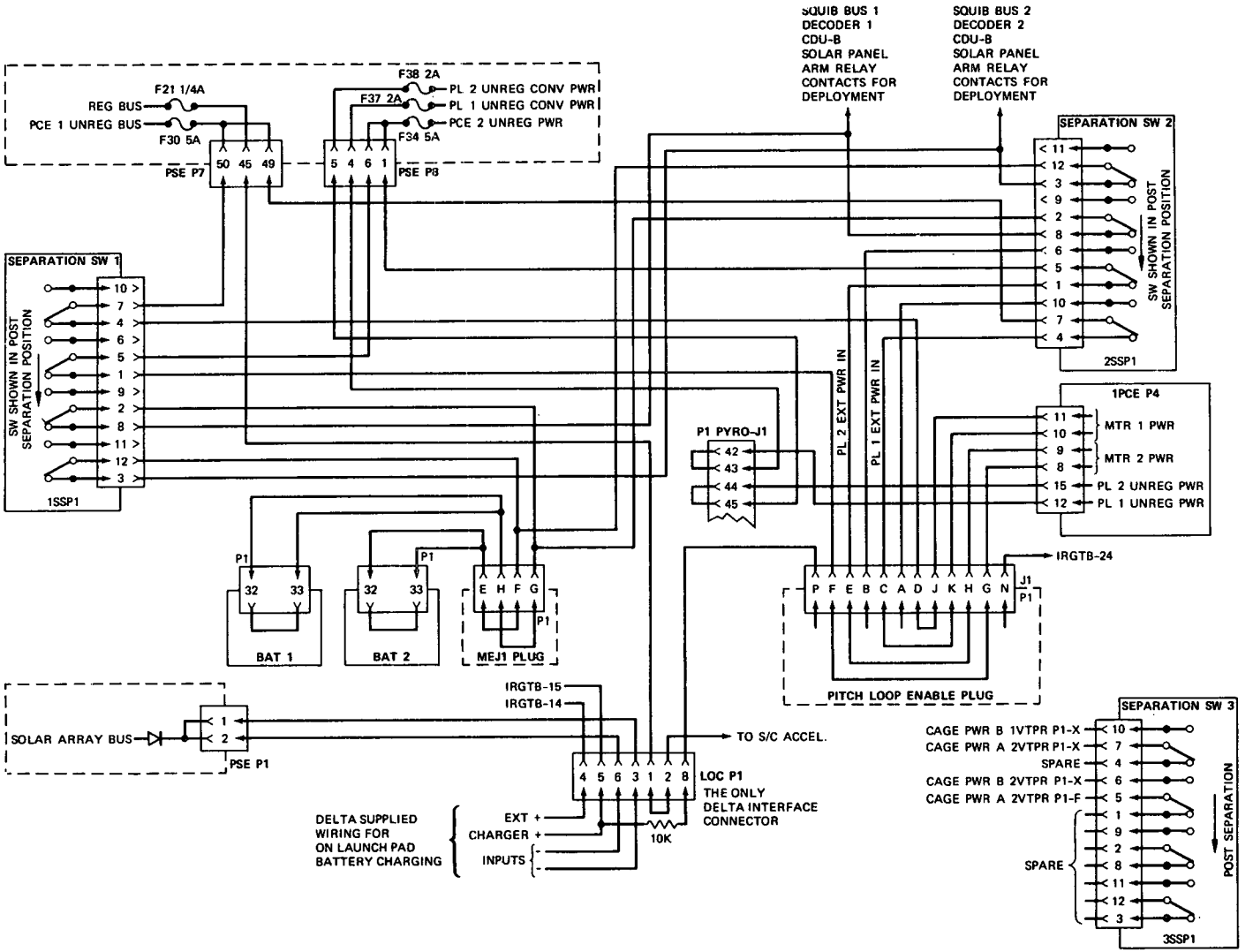

Figure 17. Interface Wiring and Separation Switch Functions

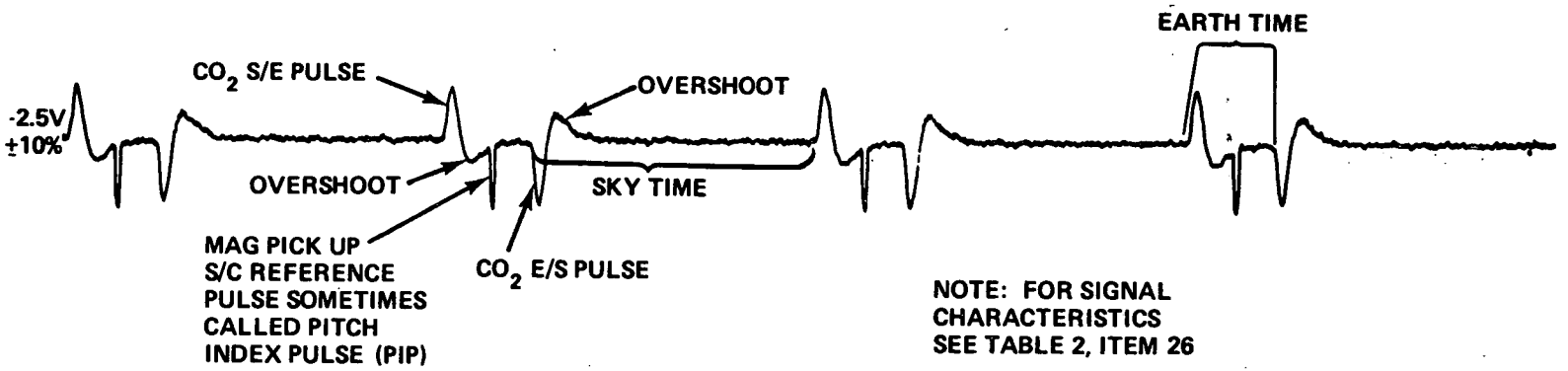

Figure 18. NOAA-2 Real-Time Beacon Telemetry Data for Pitch Loop-1 Horizon Sensor and Pitch Index

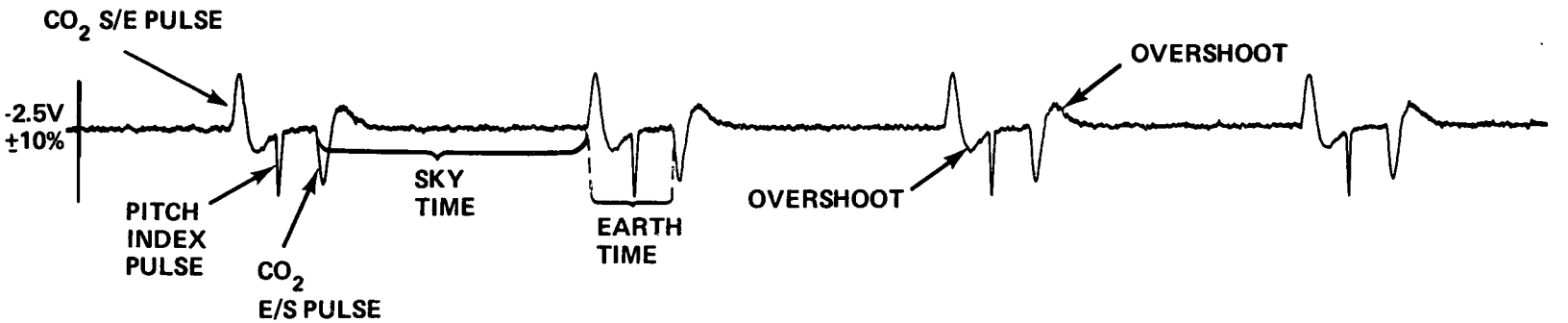

NOTE: SEE FIG. 18

Figure 19. NOAA-2 Real-Time Beacon Telemetry Data for Pitch Loop-2 Horizon Sensor and Pitch Index

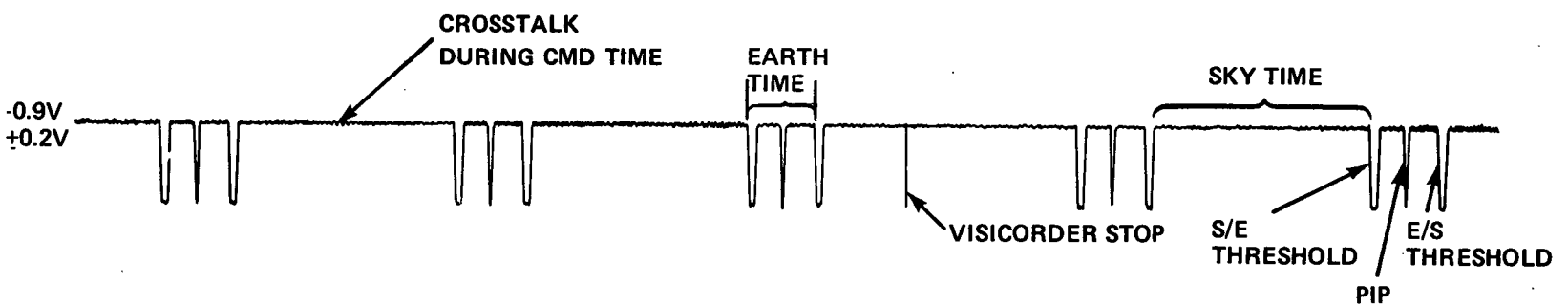

Figure 20. NOAA-2 Real-Time Beacon Telemetry Data for Pitch Loop-1 Earth Scan Data

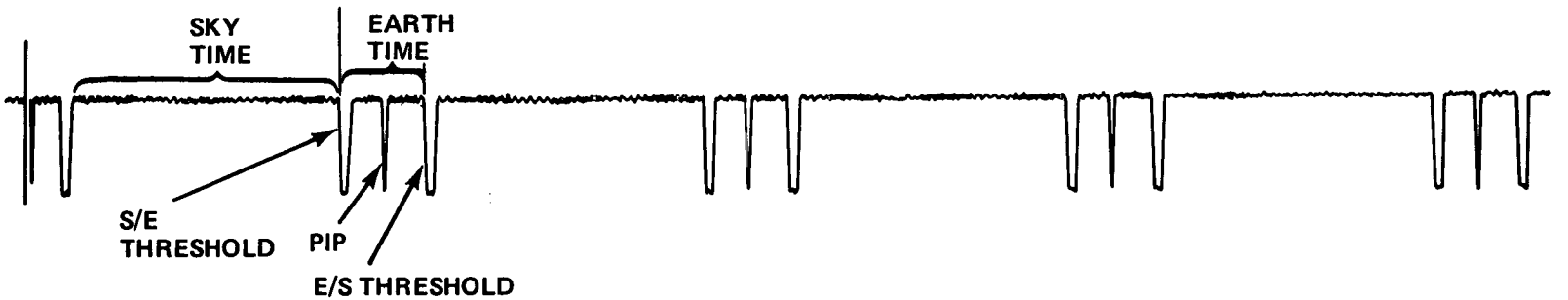

Figure 21. NOAA-2 Real-Time Beacon Telemetry Data for Pitch Loop-2 Earth Scan Data

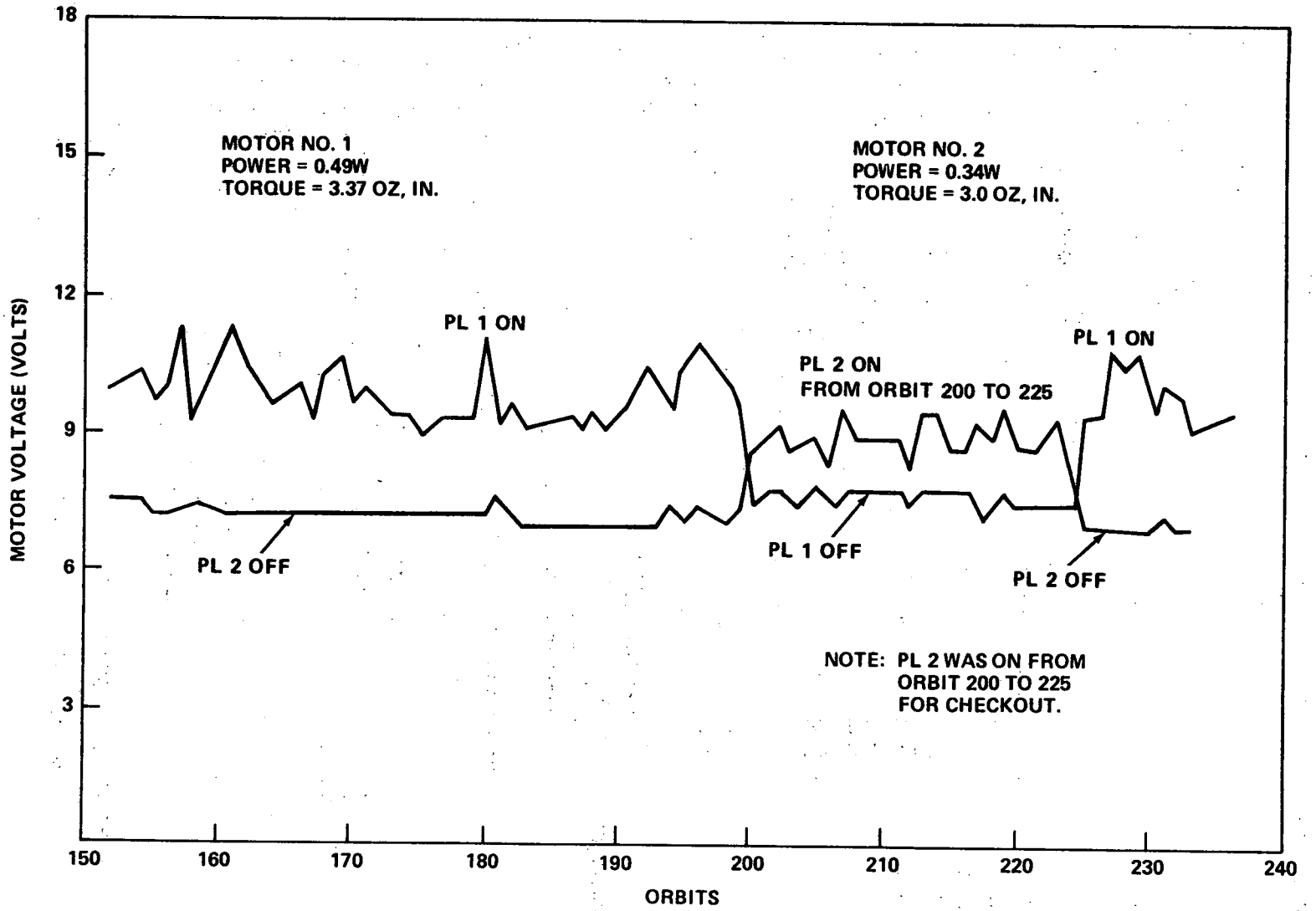

Figure 22. NOAA-2 Channels 96 and 98 Pitch Loops-1 and -2 Motor Voltage Housekeeping Telemetry TEC/GSFC, Nov. 3, 1972

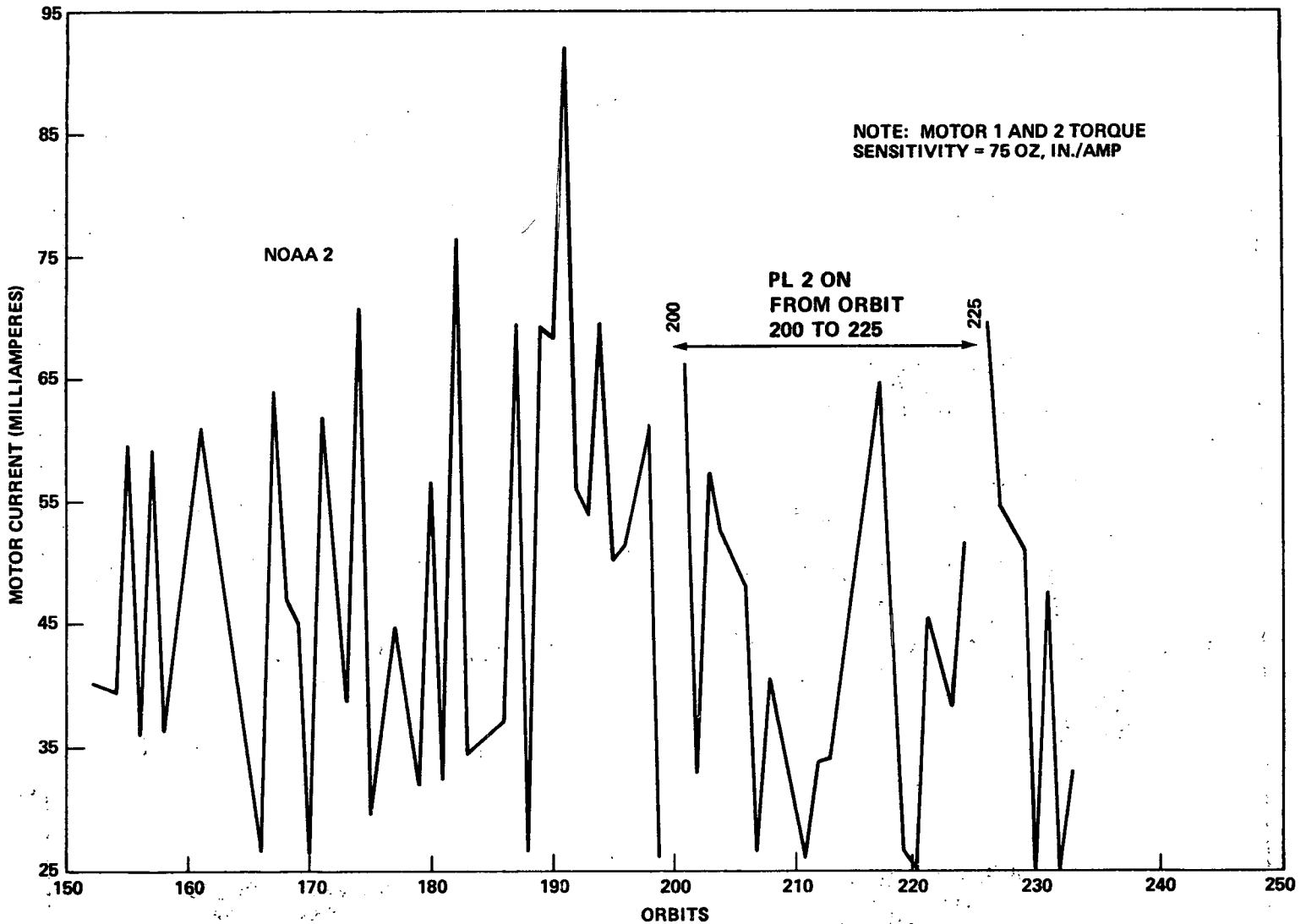

Figure 23. NOAA-2 Channels 95 and 97 Pitch Loops-1 and -2 Motor Current Housekeeping Telemetry TEC/GSFC, Nov. 3, 1972